Energy Economics 85 (2020) 104495

Contents lists available at ScienceDirect

Energy Economics

journal homepage: www.elsevier.com/locate/eneeco

Does bulk electricity storage assist wind and solar in replacing dispatchable power production?

Martin Christoph Soini*, David Parra, Martin Kumar Patel

Energy Efficiency Group, Institute for Environmental Sciences, University of Geneva, 66 Boulevard Carl-Vogt, 1205, Switzerland

ARTICLE INFO

Article history:
Received 23 January 2019
Received in revised form 9 August 2019
Accepted 15 August 2019
Available online 22 August 2019

Keywords:
Impact of bulk storage on electricity systems
Expansion of wind and solar power
Emissions from electricity production
De-carbonization of power supply

ABSTRACT

This paper discusses the impact of bulk electric storage on the production from dispatchable power plants for rising variable renewable electricity shares. Two complementary optimization frameworks are used to represent power systems with a varying degree of complexity. The corresponding models approximate the wholesale electricity market, combined with the rational retirement of dispatchable capacity. Two different generic storage technologies are introduced exogenously to assess their impact on the system.

The analysis covers two countries: France, where the power supply's large nuclear share allows for the discussion of storage impact on a single generator type; and Germany, whose diverse power supply structure enables storage interactions with multiple electricity generators. In the most general case, additional storage capacity increases dispatchable power production (e.g. nuclear, coal) for small wind and solar shares, i.e. it compensates the replacement induced by renewable energies. For larger variable renewable electricity volumes, it actively contributes to dispatchable power replacement. In a diverse power system, this results in storage-induced sequential mutual replacements of power generation from different plant types, as wind and solar capacities are increased.

This mechanism is strongly dependent on the technical parameters of the storage assets. As a result, the impact of different storage types can have opposite signs under certain circumstances. The influence of CO_2 emission prices, wind and solar profile shapes, and power plant ramping costs is discussed.

1. Introduction

To decarbonize the electricity sector, wind and photovoltaic (PV) power are likely to cover increasing shares of future electricity production (Creutzig et al., 2017; Luderer et al., 2017). To cope with the inherently variable nature of these renewable resources, their integration requires additional system flexibility (International Energy Agency, 2018). This flexibility is necessary in order to follow steeper load ramps (Huber et al., 2014), to manage short-term power fluctuations (International Energy Agency, 2018), and to counteract the market value erosion of resources with inflexible profiles (Hirth, 2013). Ultimately, very high shares of variable renewable electricity (VRE) require the system to absorb otherwise curtailed peak generation (Denholm and Hand, 2011; Després et al., 2017).

The future needs for additional flexibility of supply and demand can be satisfied in a multitude of ways, relying both on improvements of the legacy system (such as power plant upgrades (International Energy Agency, 2018)) and on dedicated measures, including storage installation and cross-sector coupling (Lund et al., 2015). Among these options, electricity-to-electricity storage stands out as especially versatile due its ability to provide a multitude of (e.g. ancillary) services and due to its lack of scalability constraints (with the notable exception of pumped hydro storage—PHS) (Fitzgerald et al., 2015; Palizban and Kauhaniemi, 2016). This is in addition to several more technology-specific advantages like estimated low capital costs per energy capacity (e.g. compressed air energy storage (Lazard, 2016)), pronounced anticipated cost decreases (e.g. battery technologies (Schmidt et al., 2017)), very fast deployment time, modularity, and increasing maturity due to rapidly accelerating worldwide use (batteries (REN21, 2018; Tortora, 2014)).

Current trends speak for a strong future build-out of storage capacity: Policies around the world aim at mandating, incentivizing, or facilitating the installation of these assets (REN21, 2018; State of California, 2010). Increasing production volumes (not least due to the rising demand from other sectors, e.g. the automotive industry) have allowed (Nykvist and Nilsson, 2015) and are likely to continue to allow (Schmidt et al., 2017) for substantial cost decreases.

* Corresponding author.
E-mail addresses: martin.soini@unige.ch (M.C. Soini), david.parra@unige.ch (D. Parra), martin.patel@unige.ch (M.K. Patel).

https://doi.org/10.1016/j.eneco.2019.104495
0140-9883/

While the current economics of grid-connected storage performing pure energy time-shifting is often found to be unfavorable (Soini et al., 2019; Wilson et al., 2018), these assets are inherently able to tap into multiple revenue streams (transmission and distribution investment deferral, provision of reserve capacity, regulation, etc.) (Fitzgerald et al., 2015; Stephan et al., 2016). In this way, profit from energy trading on the wholesale market is not the sole factor justifying the installation of storage capacity. Furthermore, the ongoing build-out of VRE promises a future increase of storage operation profits (Hartner and Permoser, 2018).

The estimated volumes of future storage demand are substantial. In a meta-analysis of 17 studies for the United States, Europe (aggregated), and Germany, Cebulla et al. found that the need for storage power and energy capacities increases strongly for rising VRE shares (Cebulla et al., 2018). Thereby, required storage capacities are especially high for large shares of PV power production, as compared to wind. In the German case, energy capacities vary strongly, yet are concentrated between 50 and 150 GWh for VRE shares up to 60%. This corresponds to 0.008–0.023% of the 2015 gross electricity demand (German Federal Ministry for Economic Affairs and Energy (BMWi), 2018).

As evidenced by this research, storage can be expected to play a much more pronounced role in future power systems. This is due to the wide range of drivers for storage capacity expansion, the large technological diversity of these assets, as well as their breadth of use. However, considerable uncertainty remains with respect to volumes and types: In most cases, a focus on storage as an enabling technology for the VRE build-out is a design choice. This justifies the study of storage impact on the power supply.

Studies within the current body of literature discuss various aspects of systemic storage impacts. The emissions impact of storage capacity operating as a price taker is an often-discussed topic and is potentially positive and significant (Fares and Webber, 2017; Hittinger and Azevedo, 2017). This is due to the positive correlations of low electricity prices and high power CO_2 intensities (e.g. due to coal power production at night and daytime gas power plant operation). Also for bulk storage interacting with the power system, increasing emissions were found in scenarios with low VRE shares in the Dutch grid, while larger VRE shares are associated with storage-induced emission decreases (de Boer et al., 2014). Similarly, Goteti et al. investigated the required wind and solar shares to allow bulk storage to reduce CO_2 emissions (Goteti et al., 2017). This was found to be relevant in grid regions with coal-fueled power production. Thereby, storage-induced emissions strongly depend on natural gas and carbon prices. This is corroborated by research focusing on the impact of storage in static status quo power systems *without* VRE additions: In case of a United States day-ahead energy market, Lueken and Apt found storage-induced production shifts from different power plant types, resulting in emission increases (Lueken and Apt, 2014).

Another common aspect is the impact of storage capacity as an additional asset in greenfield system optimizations. Storage is found to increase (Brouwer et al., 2016; de Sisternes et al., 2016) or decrease (Bussar et al., 2016) total system cost depending on the technical parameters and the reference case definition. Also, storage-induced shifts of the least cost system composition toward higher wind and solar shares have been reported (de Sisternes et al., 2016). A number of studies optimize the installed storage capacity, but discuss scenarios where this additional investment is constrained (Babrowski et al., 2016; Schill and Zerrahn, 2018).

1.1. Research question and outline

All things equal, introducing bulk storage capacity into an electricity market has complex direct and indirect effects (Soini, 2015). While the existing literature touches on many aspects of these interactions, a more systematic analysis is missing. This paper generalizes these aspects by discussing the mechanisms behind the storage impact on conventional power generators for rising VRE shares in a simplified perfect market setting with rational retirement decisions of dispatchable capacity. It makes use of two complementary model frameworks:

- An hourly dispatch model covering five Western European countries; within each country, power plants are aggregated by fuel and represented by linear cost supply curves.
- Additionally, a stylized modeling framework is used to provide a bottom-up discussion of the relevant mechanisms.

This study makes two contributions to the literature: First, it discusses how and under which circumstances storage amplifies or compensates the VRE-induced replacement of dispatchable production. And second, it demonstrates the applicability of maximally reduced stylized models to discuss the underlying mechanisms. These models consist of the minimum number of components to reproduce the effects of interest. The outline of the remainder of this paper is shown in Fig. 1.

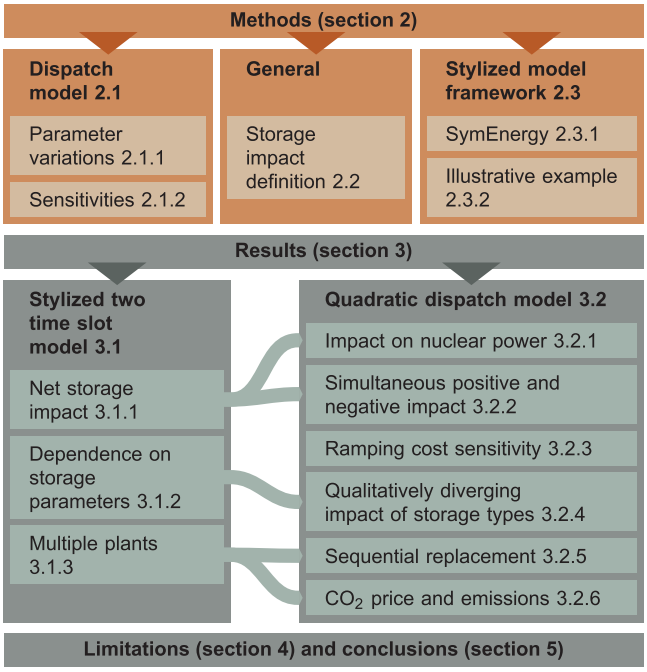

Fig. 1. Outline of the remainder of this paper. Explanatory relations between the stylized model (results Section 3.1) and the dispatch model (results Section 3.2) are indicated by arrows.

2. Methods

2.1. Quadratic dispatch model

This study relies on a stylized quadratic dispatch and capacity retirement model of the electricity supply in five countries. It approximates perfect electricity market conditions and rational retirement decisions by minimizing variable and fixed costs while satisfying inelastic hourly demand. The optimization has perfect foresight. Reserve markets and other ancillary services are not considered. The endogenous variables cover the power plant and storage operation, direct current transmission between copperplate countries, as well as power plant capacity retirements. A single year is represented by the set $\mathcal{H}$ of its 8760 hours t. The limitation to a single year entails the implicit assumption that this

Table 1
Exogenous net legacy capacity (GW) installed in the reference year 2015. The column *Retire* indicates whether the capacities can be endogenously retired by the optimizer. Data sources are documented in the supplementary material, section D.

	AT	FR	DE	IT	CH	Retire
Reservoirs	3.99	8.21	1.54	13.22	7.56	No
Run-of-river	5.66	10.32	3.84	5.20	4.16	No
PHS	4.00	4.96	8.15	3.80	1.90	No
Biomass	0.62	0.92	7.47	2.98	0.05	No
Waste	0.37	0.78	1.92	0.92	0.44	No
Geothermal	-	-	-	0.77	-	No
Nuclear	-	63.13	10.80	-	3.33	Yes
Natural gas	4.60	10.24	24.04	43.92	0.31	Yes
Hard coal	1.10	3.01	24.61	8.70	-	Yes
Lignite	-	-	20.68	-	-	Yes
Mineral oil	0.17	8.50	4.20	3.20	0.07	No

particular year repeats endlessly. The detailed mathematical model description is provided in the supplementary material (section C). The modeling framework, input data, and the script to replicate all model runs are available online.[1]

The model includes Austria (AT), France (FR), Germany (DE), Italy (IT), and Switzerland (CH). Each of these countries is represented by a single node, i.e. national transmission grids are neglected. Cross-border power exchange is constrained by exogenous historic net transfer capacities, which are defined as averages for each month of the year.

Legacy power plant capacities of the reference year 2015 are included in the model at zero capital cost (see Table 1). Because of this, the composition of the generator fleet is largely determined by the status quo together with the exogenously defined VRE expansion. However, adjustments to the dispatchable plants are possible: Their capacity can be reduced if their yearly net value is lower than their fixed operations and maintenance (O&M) costs. This study's focus lies on the replacement of incumbent dispatchable power production and capacity with additional VRE; because of this, endogenous investments in new power plant capacity are not considered.

Specific variable costs are expressed as linear functions. This parameterizes the aggregated power plants' output-dependent efficiency: All things equal, the units with the lowest efficiency $\eta_{\mathrm{pp,min}}$ ($\mathrm{MWh_{el}/MWh_{fuel}}$) will incur the greatest variable costs for fuels and CO_2 emissions per unit of produced electricity. The index pp denotes the aggregated power plants. For a given power output $p_{\mathrm{pp},t}$, these specific variable costs are therefore expressed as $\gamma_{\mathrm{f}}\left(\nu_{0,\mathrm{pp}} + p_{\mathrm{pp},t}\,\nu_{1,\mathrm{pp}}\right)$, with specific fuel costs γ_{f} ($\mathrm{EUR/MWh_{fuel}}$).[2] The factors $\nu_{0,\mathrm{pp}} = 1/\eta_{\mathrm{pp,max}}$ and $\nu_{1,\mathrm{pp}} = (1/\eta_{\mathrm{pp,min}} - 1/\eta_{\mathrm{pp,max}})\Gamma_{\mathrm{pp}}{}^{-1}$ follow from the properties (efficiencies and installed capacity Γ_{pp}) of each power plant type in each country in the reference year 2015. The total cost supply curves resulting from this approach are shown in Fig. 2.

Both the hourly demand and the VRE supply are modeled through equality constraints; however, power production can be curtailed through a dedicated technology. Additional power plant inflexibilities are the following:

- The must-run conditions of co-generation plants $p_{\mathrm{pp},t} \geqslant \Phi_{\mathrm{CHP,pp},t}$ are implemented by means of a temperature-dependent and country-specific power production profile $\Phi_{\mathrm{CHP,pp,t}}$. This profile is scaled in order to satisfy the 2015 power production from co-generation units for each power plant type and country. It is fixed for all model runs.

Table 2
Parameters of battery-type short-term storage (STS) and PHS-type long-term storage (LTS). The power capacity is expressed as a fraction (MW/MW) of average demand in each country. The energy capacity is added for comparison. It is expressed as a fraction (MWh/MWh) of the total electricity demand and follows from the power capacity share and the discharge duration.

	LTS	STS
Round-trip efficiency (%)	75	90
Discharge duration (h)	20	4
Power capacity σ(%)	0...30	0...30
Energy capacity (%)	0...0.068	0...0.014

- Power output changes of dispatchable generators entail a variable cost $\gamma_{\mathrm{ramp,pp}}\left|p_{\mathrm{pp},t} - p_{\mathrm{pp},t-1}\right|$. The specific ramping costs $\gamma_{\mathrm{ramp,pp}}$ (EUR/MW) are approximated by an appropriate mix of reported financial penalties for both power plant start-ups and output level adjustments (Egerer et al., 2014) .

The minimized objective function is the sum of all system costs. It consists of the following terms:

- The quadratic variable fuel costs defined by the specific costs $\gamma_{\mathrm{f,n,m}}$ ($\mathrm{EUR/MWh_{fuel}}$); the fuels f(pp) and the countries n(pp) are functions of the power plants pp, the months m(t) are a function of the year's hour t:

$$\sum_{\mathrm{pp}}\sum_{t} p_{\mathrm{pp},t}\gamma_{\mathrm{f,n,m}}\left(\nu_{0,\mathrm{pp}} + 0.5\cdot\nu_{1,\mathrm{pp}}\cdot p_{\mathrm{pp},t}\right), \tag{1}$$

- The quadratic variable CO_2 emission costs with the emission price $\pi_{\mathrm{CO_2,n,m}}$ ($\mathrm{EUR/t_{CO_2}}$) and the emission intensity ι_{f} ($\mathrm{t_{CO_2}/MWh_{fuel}}$):

$$\sum_{\mathrm{pp}}\sum_{t} p_{\mathrm{pp},t}\pi_{\mathrm{CO_2,n,m}}\iota_{\mathrm{f}}\left(\nu_{0,\mathrm{pp}} + 0.5\cdot\nu_{1,\mathrm{pp}}\cdot p_{\mathrm{pp},t}\right), \tag{2}$$

- The variable O&M costs with specific costs $\gamma_{\mathrm{v,O\&M,pp}}$ ($\mathrm{EUR/MWh_{el}}$):

$$\sum_{\mathrm{pp}}\sum_{t} p_{\mathrm{pp},t}\cdot\gamma_{\mathrm{v,O\&\,M,pp}}, \tag{3}$$

- The variable ramping costs $\sum_{\mathrm{pp}}\sum_{t}\left|p_{\mathrm{pp},t} - p_{\mathrm{pp},t-1}\right|\gamma_{\mathrm{ramp,pp}}$,
- and the fixed O&M costs with the exogenous legacy capacity Γ_{pp}, the endogenously retired capacity $C_{\mathrm{ret,pp}}$, and the specific fixed[3] costs $\gamma_{\mathrm{f,O\&M,pp}}$ (EUR/MW/yr):

$$\sum_{\mathrm{pp}}(\Gamma_{\mathrm{pp}} - C_{\mathrm{ret,pp}})\gamma_{\mathrm{f,O\&\,M,pp}}. \tag{4}$$

2.1.1. Model parameter variations

The goal of this parameter study is the systematic exploration of storage interactions with the other power system components. Because of this, its focus lies on the disentanglement of mechanisms, rather than the analysis of future scenarios. This purpose drives the model setup and the parameter selection.

Two generic storage technologies are considered (see Table 2): high-efficiency batteries with short discharge duration (referred to as short-term storage, STS), and storage with large energy capacity yet lower round-trip efficiency (long-term storage, LTS). The latter approximates various technologies with low energy capacity capital costs, such as adiabatic compressed air or PHS.

In the dispatch model, storage provides energy time shifting services by charging and discharging during hours with low and high

[1] https://github.com/mcsoini/grimsel/tree/replace.
[2] Throughout this paper, endogenous variables and exogenous parameters are denoted by Latin and Greek letters, respectively.
[3] Fixed O&M costs for storage are not included since all storage capacity is set exogenously.

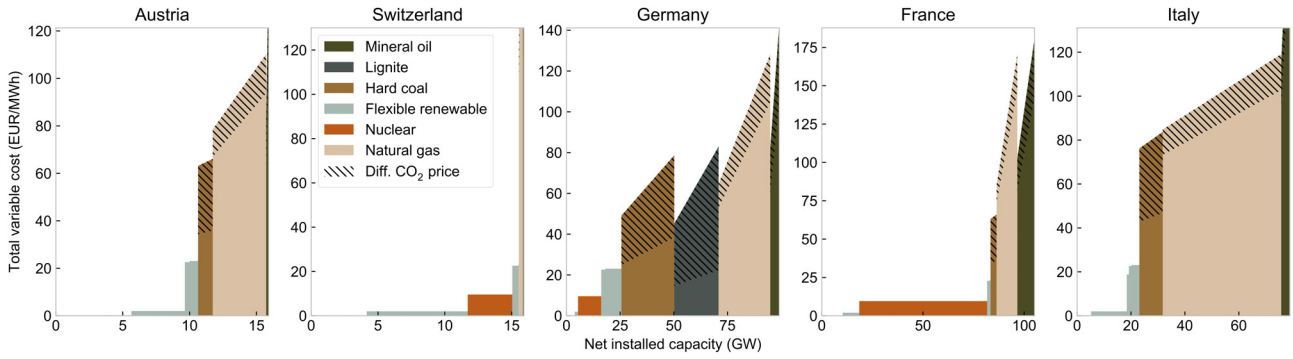

Fig. 2. Supply curves representing the power plant cost structure in the quadratic dispatch model. This includes all variable costs incurred for fuels, O&M, and CO_2 emissions. The hatched ranges correspond to the cost increase for the default CO_2 emission price of 40 EUR/t, as compared to 5 EUR/t. In the model, power plants are dispatched according to cost, independent of the order shown here.

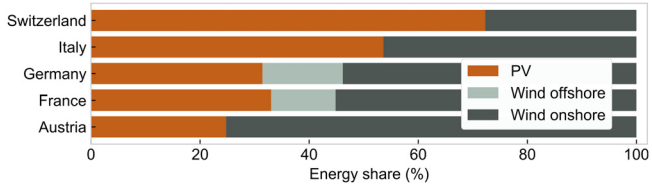

Fig. 3. Assumed composition of the default VRE production mix.

electricity value, respectively. Furthermore, storage power capacity can replace the system's legacy generators.

This study focuses on the variation of three key parameters:

- The VRE energy share μ is expressed as a fraction of total yearly demand up to 70%. It is varied in step sizes as small as 2.5%. Within this total VRE share, the relative fractions of wind and solar power are assumed to be constant (see Fig. 3). They are based on mid- to long-term scenarios (Capros et al., 2016; Prognos AG, 2012).
- The relative storage *power* capacity σ is varied between 0 and 30% of average demand in all countries (step sizes as small as 1%). The maximum corresponds to *energy* capacities between 0.014% (STS) and 0.068% (LTS) as a fraction of total annual demand (see Table 2). These storage volumes are in line with estimated future storage demands (Cebulla et al., 2018) and with assumed ranges in studies analyzing exogenous storage capacity (de Sisternes et al., 2016; Lueken and Apt, 2014; Nyamdash and Denny, 2013).
- ST and LT storage are analyzed separately. This allows to compare the impact of storage types with different technical parameters. While the assumption of a mixed storage fleet would be more realistic, the focus of this study lies on the disentanglement of storage impact mechanisms and their dependence on the storage parameters. The operation of existing PHS plants is subject to optimization. However, their capacity remains fixed at the reference year value in all model runs.

All analyzed parameter variations are based on the assumption that the respective power system changes are adopted in all countries simultaneously. Cases where country A implements vast amounts storage or variable capacity, while the neighboring country B maintains the status quo, are not considered. Also this simplification is justified by this study's exploratory nature.

2.1.2. Sensitivities

Additional model runs are performed to assess sensitivities with respect to certain parameters. This includes CO_2 emission costs, the VRE mix (pure wind or solar profiles as compared to the default mix in Fig. 3), and power plant ramping costs. In addition, the VRE profiles (hourly capacity factors) are varied by selecting different meteorological years 2011–2016. The aim is to compare the impact of the profile shape; the capacity factor of each year is normalized by iteratively adding or subtracting random normal distributions of appropriate size, to obtain a match with the reference year 2015: Starting from the original profile of an alternative year yr $\neq$ 2015, the total yearly full load hours $\sum_{t\in\mathcal{H}} \mathrm{cf}_{\mathrm{yr},t}$ and $\sum_{t\in\mathcal{H}} \mathrm{cf}_{2015,t}$ are calculated. A normal distribution (standard deviation 200 h, random mean $\in\mathcal{H}$) is generated, scaled by $\sum_t \mathrm{cf}_{2015} - \sum_t \mathrm{cf}_{\mathrm{yr},t}$, and added to the original profiles. Depending on the original profile's shape, this can lead to negative values. They are adjusted by setting the capacity factor during the corresponding hours to zero. Because of this, additional subtraction steps are required. The iteration ends as soon as the total yearly capacity factor difference is sufficiently small.

2.2. Definition of storage impact

The primary focus of this paper is the impact of storage capacity on various indicators. When applied to a quantity x, the *storage impact* operator $\Delta_{\sigma=\sigma_1}$ is defined to yield the difference between the value of x in the scenario with storage capacity $\sigma=\sigma_1$ and the reference case without additional storage capacity $\sigma=0$: $\Delta_{\sigma=\sigma_1} x = x_{\sigma=\sigma_1} - x_{\sigma=0}$. In the remainder of the paper, this is applied to produced energy ($\Delta_\sigma e$), net installed capacity ($\Delta_\sigma C$), full load hours (Δ_σFLH), and CO_2 emissions ($\Delta_\sigma E$).

2.3. Stylized model framework

Simple stylized models are employed to discuss the basic interactions of VRE, power plants, and storage. These models contain the minimum required number of power plants and time slots in order to reproduce the mechanisms of interest. Because of this simplicity, their closed-form analytical solutions can be identified, i.e. the variables can be expressed explicitly as functions of the parameters. They form a complementary approach to the dispatch model: While the latter represents the system with a fairly high detail level and temporal resolution, the stylized models allow for a bottom-up discussion of the relevant mechanisms.

2.3.1. SymEnergy

To define and solve these models, we use our framework SymEnergy[4], which is based on Python's symbolic mathematics package SymPy (Meurer et al., 2017) . SymEnergy is a straightforward implementation of the Lagrange formulation of the cost-minimization problem for energy systems. These systems con-

[4] https://github.com/mcsoini/symenergy/tree/replace.

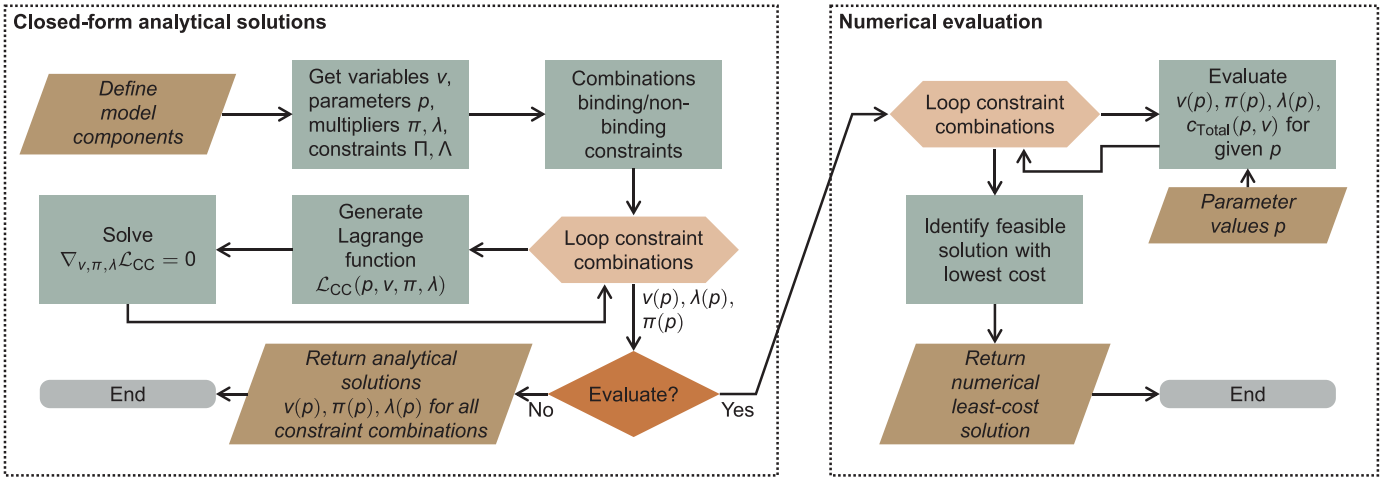

Fig. 4. Flowchart illustrating the SymEnergy solution process.

sist of arbitrary numbers of time slots, power plants, and storage units:

- Time slots t are characterized by parameters representing the demand level $\Phi_{\text{Load},t}$ and the VRE production $\Phi_{\text{VRE},t}$. Optionally, a power variable $p_{\text{Curt},t}$ allows for surplus production. These variables must be greater than zero, i.e. they are subject to positivity constraints $\Lambda_{\text{pos},p_{\text{Curt},t}} \geqslant 0$ with $\Lambda_{\text{pos},p_{\text{Curt,t}}} = p_{\text{Curt},t}$.[5]
- Power plants pp produce electric power (variable $p_{\text{pp},t}$) at a linear specific variable cost $c_{\text{v},t} = \gamma_{\text{v},0,\text{pp}} + \gamma_{\text{v},1,\text{pp}} \cdot p_{\text{pp},t}$ with parameters $\gamma_{\text{v},0,\text{pp}}$ and $\gamma_{\text{v},1,\text{pp}}$ (compare Section 2.1). Optional parameters are fixed O&M costs $\gamma_{\text{f,pp}}$ (EUR/MW) and installed capacities Γ_{pp} (MW). The optional retired capacity variable $C_{\text{pp,ret}}$ (MW) is subject to optimization. The total cost associated with power plant operation is thus

$$c_{\text{Total}} = \sum_{\text{pp},t} [p_{\text{pp},t}(\gamma_{\text{v},0,\text{pp}} + 0.5 \cdot \gamma_{\text{v},1,\text{pp}} \cdot p_{\text{pp},t}) + \gamma_{\text{f,pp}}(\Gamma_{\text{pp}} - C_{\text{pp,ret}})]. \tag{5}$$

  The feasible solution space is reduced by the capacity constraints $\Lambda_{\text{cap},p_{pp,t}} = (\Gamma_{pp} - C_{pp,ret}) - p_{pp,t} \geqslant 0$ and $\Lambda_{\text{cap},C_{pp,re,t}} = \Gamma_{pp} - C_{pp,ret} - \geqslant 0$, as well as the positivity constraints $\Lambda_{\text{pos},p_{\text{pp},t}} = p_{\text{pp},t} \geq 0$ and $\Lambda_{\text{pos},C_{\text{pp,ret}}} = C_{\text{pp,ret}} \geq 0$.
- Storage assets s charge and discharge with power $p_{\text{chg/dch,s,t}}$.[6] The maximum stored energy e_{s} is a variable. Power and energy are subject to positivity constraints and optional capacity constraints (power capacity Γ_{s} and energy capacity Σ_{s}), analogous to the power plant variables.

  Energy conservation is enforced through the charging-discharging equality constraint $\Pi_{\text{cd,s}} = \sum_t p_{\text{chg,s,t}}\eta_{\text{s}} - \sum_t p_{\text{dch,s,t}} = 0$ (round-trip efficiency η_{s}); the charged energy follows from $\Pi_{\text{e,s}} = \sum_t p_{\text{chg,s,t}}\eta_s^{1/2} - e_{\text{s}} = 0$.

For each t, the demand constraint is defined as $\Pi_{\text{d},t} = \Phi_{\text{Load},t} + p_{\text{Curt},t} + \sum_{\text{s}} p_{\text{chg,s,t}} - \Phi_{\text{VRE},t} - \sum_{\text{s}} p_{\text{dch,s,t}} - \sum_{\text{pp}} p_{\text{pp},t} = 0$.

With the supply curves being linear, the total cost function in Eq. (5) is quadratic. Therefore, the Karush-Kuhn-Tucker (KKT) conditions $\nabla_{\boldsymbol{v},\boldsymbol{\pi},\boldsymbol{\lambda}}\mathcal{L}_{CC} = 0$ form a system of linear equations, whose closed-form analytical solutions $\boldsymbol{v}(\boldsymbol{p})$, $\boldsymbol{\pi}(\boldsymbol{p})$, and $\boldsymbol{\lambda}(\boldsymbol{p})$ can be calculated. Thereby, $\boldsymbol{p}$, $\boldsymbol{v}$, $\boldsymbol{\pi}$, and $\boldsymbol{\lambda}$ are the vectors of all parameters and variables, as well as the multipliers of the equality (Π) and inequality constraints (Λ), respectively. The Lagrange functions $\mathcal{L}_{CC}$ are generated for each of the possible combinations CC of the n_Λ binding or non-binding inequality constraints Λ. For example, two inequality constraints Λ_1 and Λ_2 require the definition of four constraint combinations defined by $(\Lambda_1, \Lambda_2) \in \{(0,0), (\mathbb{R}_{>0}, 0), (0, \mathbb{R}_{>0}), (\mathbb{R}_{>0}, \mathbb{R}_{>0})\}$. In the general case this yields

$$\mathcal{L}_{CC}(\boldsymbol{p}, \boldsymbol{v}, \boldsymbol{\pi}, \boldsymbol{\lambda}) = c_{\text{Total}} \quad (\boldsymbol{p}, \boldsymbol{v}) + \sum_i \pi_i \Pi_i(\boldsymbol{p}, \boldsymbol{v}) + \sum_j \lambda_j \Lambda_{j,CC}(\boldsymbol{p}, \boldsymbol{v}), \tag{6}$$

including all binding inequality expressions $\Lambda_{\text{j,CC}}(\boldsymbol{p}, \boldsymbol{v}) = 0$. The solutions $(\boldsymbol{v}, \boldsymbol{\pi}, \boldsymbol{\lambda})$ of the 2^{n_Λ} constraint combinations are candidates for the cost minimization. Based on plausibility considerations, the vast majority of combinations can be excluded prior to solving. The solution process is illustrated as a flow chart in Fig. 4. A basic example is discussed in Section 2.3.2.

2.3.2. Illustrative example

In this section, a basic example is used to demonstrate the optimization using SymEnergy. The considered system is simple enough for its optimal solution to be intuitively accessible. Energy is supplied during a single time slot (load parameter Φ_{Load}, VRE production parameter Φ_{VRE}) by cheap baseload power and expensive peaker plants:

- Baseload production p_{Base} (specific variable cost γ_{Base}) must be positive (constraint $\Lambda_{\text{pos},p_{\text{Base}}} \geqslant 0$, multiplier $\lambda_{\text{pos},p_{\text{Base}}}$); it is constrained by the baseload capacity Γ_{Base} ($\Lambda_{\text{cap},p_{\text{Base}}} \geqslant 0$ with multiplier $\lambda_{\text{cap},p_{\text{Base}}}$).
- Peaker plant production p_{Peak} (specific variable cost $\gamma_{\text{Peak}} > \gamma_{\text{Base}}$) must be positive ($\Lambda_{\text{pos},p_{\text{Peak}}} \geqslant 0$, multiplier $\lambda_{\text{pos},p_{\text{Peak}}}$) and is otherwise unconstrained.

The total cost is $p_{\text{Base}}\gamma_{\text{Base}} + p_{\text{Peak}}\gamma_{\text{Peak}}$, the demand constraint is $\Pi_{\text{d}} = \Phi_{\text{Load}} - p_{\text{Base}} - p_{\text{Peak}} - \Phi_{\text{VRE}} = 0$ with multiplier π_{d}.

Without further analysis, the optimal solution can be expected to correspond to the case where p_{Base} covers a maximum of the residual load $\Phi_{\text{Load}} - \Phi_{\text{VRE}}$, with p_{Peak} supplying the rest. This is shown in Fig. 5a as a function of the VRE share. SymEnergy starts from the 3 binding or non-binding inequality constraints. Conse-

[5] Equality constraint expressions are denoted by Π, inequality constraint expressions are represented by the symbol Λ.

[6] In the SymEnergy models defined for this study, the time slots during which storage charges and discharges are defined a priori, i.e. charging only happens during daytime, discharging is limited to nighttime. This allows to reduce the number of variables. Care is taken not to exclude any optimal solutions due to this choice.

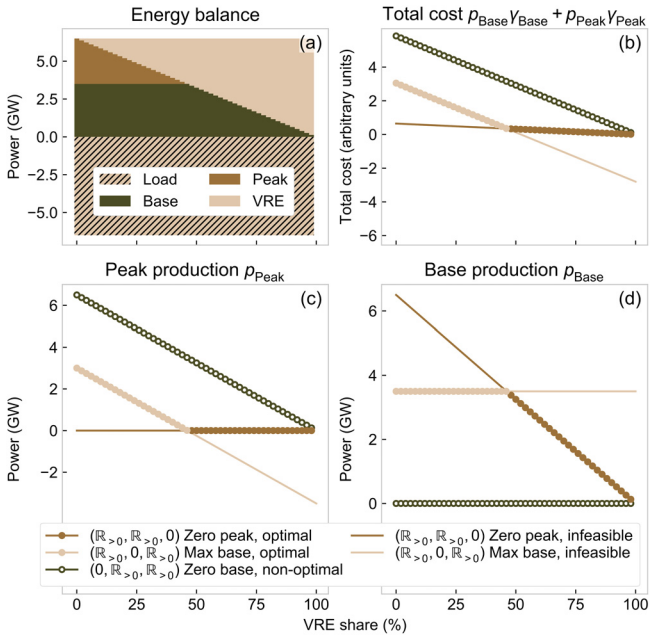

Fig. 5. Example of the optimal solution's construction from all feasible constraints combinations. Panel a: Optimal energy balance as a function of the VRE share (steps: $\Delta\mu = 2\%$). The optimized variable values (output from power plants, panels c and d) follow from the comparison of the feasible solutions' total costs (panel b). The tuples $(\mathbb{R}_{>0}, \mathbb{R}_{>0}, 0)$ etc. in the legend correspond to the combinations of active and inactive constraints defined in Eq. (7).

quently, the total number of potential general solutions (constraint combinations) is $2^3 = 8$:

- Two of these constraint combinations—$(\Lambda_{\text{pos},p_{\text{Base}}}, \Lambda_{\text{cap},p_{\text{Base}}}, \Lambda_{\text{pos},p_{\text{Peak}}}) \in \{(0,0,\mathbb{R}_{>0}), (0,0,0)\}$—correspond to the case where baseload power production is simultaneously zero and equal its installed power capacity. They can be excluded a priori, without loss of generality.
- Three of the remaining constraints would be valid only for specific parameter value combinations. For example, all constraint combinations with zero peakload production and binding baseload capacity constraint ($\Lambda_{\text{pos},p_{\text{Peak}}} = \Lambda_{\text{cap},p_{\text{Base}}} = 0$), would require the baseload capacity parameter to be exactly equal the residual load parameter: $\Gamma_{\text{Base}} \equiv \Phi_{\text{Load}} - \Phi_{\text{VRE}}$. Therefore, no general solution exists.
- The remaining three combinations

$$(\Lambda_{\text{pos},p_{\text{Base}}}, \Lambda_{\text{cap},p_{\text{Base}}}, \Lambda_{\text{pos},p_{\text{Peak}}}) \in \{(\mathbb{R}_{>0}, \mathbb{R}_{>0}, 0), (\mathbb{R}_{>0}, 0, \mathbb{R}_{>0}), (0, \mathbb{R}_{>0}, \mathbb{R}_{>0})\} \quad (7)$$

are potentially optimal solutions, depending on the parameter values.

For illustration, the solution for the constraint combination $(\mathbb{R}_{>0}, 0, \mathbb{R}_{>0})$ is calculated. It implies a binding baseload capacity constraint ($\Lambda_{\text{cap},p_{\text{Base}}} = \Gamma_{\text{Base}} - p_{\text{Base}} = 0$) and both plants producing positive power output ($\Lambda_{\text{pos},p_{\text{Base}}} = p_{\text{Base}} > 0$, $\Lambda_{\text{pos},p_{\text{Peak}}} = p_{\text{Peak}} > 0$). The resulting Lagrange function is

$$\mathcal{L}_{(\mathbb{R}_{>0},0,\mathbb{R}_{>0})} = p_{\text{Base}}\gamma_{\text{Base}} + p_{\text{Peak}}\gamma_{\text{Peak}} + \lambda_{\text{cap},p_{\text{Base}}}\Lambda_{\text{cap},p_{\text{Base}}} + \pi_{\text{d}}\Pi_{\text{d}} \quad (8)$$

The KKT conditions $\nabla_{\upsilon,\pi,\lambda}\mathcal{L}_{(\mathbb{R}_{>0},0,\mathbb{R}_{>0})}(p,\upsilon,\pi,\lambda)$ with respect to all variables and multipliers yield a system of linear equations:

$$\begin{bmatrix} 0 & 0 & 1 & 1 \\ 0 & 0 & 1 & 0 \\ 1 & 0 & 0 & 0 \\ 1 & 1 & 0 & 0 \end{bmatrix} \cdot \begin{bmatrix} p_{\text{Base}} \\ p_{\text{Peak}} \\ \pi_{\text{d}} \\ \lambda_{\text{cap},p_{\text{Base}}} \end{bmatrix} = \begin{bmatrix} \gamma_{\text{Base}} \\ \gamma_{\text{Peak}} \\ \Gamma_{\text{Base}} \\ \Phi_{\text{Load}} - \Phi_{\text{VRE}} \end{bmatrix}. \quad (9)$$

Its closed-form analytical solution $p_{\text{Base}} = \Gamma_{\text{Base}}$, $p_{\text{Peak}} = \Phi_{\text{Load}} - \Phi_{\text{VRE}} - \Gamma_{\text{Base}}$, $\pi_{\text{d}} = \gamma_{\text{Peak}}$, $\lambda_{\text{cap},p_{\text{Base}}} = \gamma_{\text{Base}} - \gamma_{\text{Peak}}$ corresponds to the case where the baseload plants are operating at the capacity limit, and the peaker plant is used to cover the remaining residual load. With the respective definitions of the other Lagrange functions $\mathcal{L}_{\text{CC}}$, the general solutions for the remaining constraint combinations (Eq. (7)) are found analogously.

In Fig. 5 b–d, the solutions of all constraint combinations are evaluated for 51 discrete VRE production values from 0 to Φ_{Load}.

- **Optimal:** By definition, the optimal solution for each set of parameter values is determined by the feasible solution with the lowest total cost (panel b). For low VRE shares, this implies maximum baseload operation—$(\mathbb{R}_{>0}, 0, \mathbb{R}_{>0})$; meanwhile, peaker plants cover the remaining power demand. For higher VRE shares, the residual demand is smaller than the baseload capacity, such that the output from the latter gradually decreases; in this case, the peakload output is zero and the baseload plant is not capacity constrained—$(\mathbb{R}_{>0}, \mathbb{R}_{>0}, 0)$.
- **Non-optimal:** Another feasible solution exists for all VRE shares—$(0, \mathbb{R}_{>0}, \mathbb{R}_{>0})$: It corresponds to the baseload plant delivering zero output and all demand being covered by the peaker plants (panel c). The higher variable cost of the latter makes this option prohibitively expensive in all cases.
- **Infeasible:** Finally, the constraint combinations comprising the optimal solutions can also be infeasible, depending on the VRE share: At high VRE shares, this is the case if the baseload plants produce at full power output and peaker plants produce negative output to compensate for the overproduction. At low VRE shares, baseload plant capacity violations are equally cost-effective yet infeasible. For any given parameter set, these infeasible solutions must be identified by evaluating all of the model's constraints.

3. Results

In the results section we first discuss the basic interaction mechanisms using the stylized modeling framework (Section 3.1). Then we demonstrate their applicability in the more detailed dispatch model (Section 3.2).

3.1. Stylized two time slot model

Based on the general SymEnergy framework (Section 2.3), a stylized model with two time slots and two generating plants is defined. The time slot *day* has higher demand but 10 times higher VRE production than the time slot *night*. This corresponds to a PV-rich setting. Storage charges during the day and discharges at night, exclusively. The model components are specified in Table 3.

By design, the stylized models' least cost solutions can be described as the combination of binding and non-binding constraints (Section 2.3.2). The two time slot model defined in Table 3 has 2^{16} constraint combinations. The SymEnergy evaluation identifies 15 of them as relevant for the chosen parameters (see columns in Table 4). Their identification is based on the exact same procedure as explained for the illustrative example (Section 2.3.2). These 15 combinations define the cost minimized solution depending on the VRE share, the baseload capacity, and the storage parameters.

Table 3
Configuration of the stylized model analyzed in Section 3.1. The constraint expressions Λ are further described in Section 2.3.1. The VRE production parameter Φ_{VRE} is varied as a share of the total demand; the table entries define the relative production during the two time slots.

(a) Assets		Baseload plants	Peaker plants	Storage
$\gamma_{v,0}$	(EUR/MWh)	10	90	–
$\gamma_{v,1}$	(EUR/MWh)	0	0	–
$\gamma_{f,O\&M}$	(EUR/kW/yr)	40	–	–
Γ_{pp}	(GW)	2/4.6/5	–	0-50% of max load
Σ_{pp}/Γ_{pp}	(hours)	–	–	14 (LTS)/4(STS)
η	(%)	–	–	75/90
Power capacity constraint		$\Lambda_{cap,p_{Base,day/night}}$	–	$\Lambda_{cap,p_{Store,day/night}}$
Power positivity constraint		$\Lambda_{pos,p_{Base,day/night}}$	$\Lambda_{pos,p_{Peak,day/night}}$	$\Lambda_{pos,p_{Store,day/night}}$
Stored energy cap. constraint		–	–	$\Lambda_{cap,e_{Store}}$
Stored energy pos. constraint		–	–	$\Lambda_{pos,e_{Store}}$
Capacity retirement cap. constraint		$\Lambda_{cap,C_{Base,ret}}$	–	–
Capacity retirement pos. constraint		$\Lambda_{pos,C_{Base,ret}}$	–	–
(b) Time slots	Slot 'day'	Slot 'night'		
Φ_{Load}	(MW)	6500	5200	
Φ_{VRE}	(relative)	10	1	
Curtailment positivity constraint		$\Lambda_{pos,p_{Curt,day}}$	$\Lambda_{pos,p_{Curt,night}}$	

Table 4
Definition of the relevant combinations (columns) of binding (•) and non-binding (○) constraints. The combinations W-Z correspond to the no-storage reference case. The constraint combinations are further interpreted in Table 5. The storage impact for these constraint combinations is shown in Fig. 6.

Constraint name	Symbol	A	B	C	C^e	D	D^e	E	F	F^e	G	G^e	W	X	Y	Z
Zero baseload production day	$\Lambda_{pos,p_{Base,day}}$	○	○	○	○	•	•	○	○	○	•	•	○	•	•	○
Zero baseload production night	$\Lambda_{pos,p_{Base,night}}$	○	○	○	○	○	○	○	○	○	○	○	○	○	○	○
Zero baseload retirement	$\Lambda_{pos,C_{Base,ret}}$	•	•	•	•	•	•	○	○	○	○	○	•	•	○	○
Capacity constraint baseload power day	$\Lambda_{cap,p_{Base,day}}$	•	•	○	○	○	○	•	○	○	○	○	○	○	○	○
Capacity constraint baseload power night	$\Lambda_{cap,p_{Base,night}}$	•	•	•	•	•	•	•	•	•	•	•	•	•	•	•
Complete baseload retirement	$\Lambda_{cap,C_{Base,ret}}$	○	○	○	○	○	○	○	○	○	○	○	○	○	○	○
Peak power zero day	$\Lambda_{pos,p_{Peak,day}}$	○	•	•	•	•	•	•	•	•	•	•	•	•	•	•
Peak power zero night	$\Lambda_{pos,p_{Peak,night}}$	○	○	○	○	○	○	•	•	•	•	•	○	○	•	•
Zero storage power day	$\Lambda_{pos,p_{Store,day}}$	•	○	○	○	○	○	○	○	○	○	○	•	•	•	•
Zero storage power night	$\Lambda_{pos,p_{Store,night}}$	•	○	○	○	○	○	○	○	○	○	○	•	•	•	•
Zero stored energy	$\Lambda_{pos,e_{Store}}$	•	○	○	○	○	○	○	○	○	○	○	•	•	•	•
Capacity constraint storage power day	$\Lambda_{cap,p_{Store,day}}$	○	○	•	○	•	○	○	•	○	•	○	○	○	○	○
Capacity constraint storage power night	$\Lambda_{cap,p_{Store,night}}$	○	○	○	○	○	○	○	○	○	○	○	○	○	○	○
Capacity constraint stored energy	$\Lambda_{cap,e_{Store}}$	○	○	○	•	○	•	○	○	•	○	•	○	○	○	○
Zero curtailment day	$\Lambda_{pos,p_{Curt,day}}$	•	•	•	•	○	○	•	•	•	○	○	•	○	○	•
Zero curtailment night	$\Lambda_{pos,p_{Curt,night}}$	•	•	•	•	•	•	•	•	•	•	•	•	•	•	•

Table 5
Description of the relevant constraint combinations defined in Table 4. The combinations W-Z correspond to the no-storage reference case.

A	Storage idle; VRE replaces peakload
B	Charging from baseload to replace nighttime peakload production; no daytime peakload production
C	Charging power is capacity constrained; daytime charging increasingly from VRE
C^e	Same as C, but stored energy is capacity constrained.
D	Charging power is capacity constrained; all charging from otherwise curtailed VRE $\rightarrow \Delta_\sigma e_{Base} = 0$.
D^e	Same as D, but stored energy is capacity constrained.
E	No peaker plants left; baseload capacity factor optimization
F	Same as E, but charging power is capacity constrained.
F^e	Same as E, but stored energy is capacity constrained.
G	No peaker plants; charging only from VRE; no daytime baseload production
G^e	Same as G, but stored energy is capacity constrained.
W	No storage case; VRE fully replaces peaker plants during the day, increasingly replaces baseload.
X	No storage case; VRE supplies all energy during the day $\rightarrow$ increasing curtailment.
Y	No storage case; same as W, plus VRE fully replaces peaker plants at night.
Z	No storage case; same as X, plus VRE fully replaces peaker plants at night.

Eleven of them are relevant in the presence of storage capacity, four are exclusively part of the reference case without storage. The constraint combination A corresponds to idling storage and is relevant in both cases. All combinations are defined and described in the Tables 4 and 5.

3.1.1. Net impact of storage

Fig. 6 shows the dispatch and the LTS impact $\Delta_\sigma e$ in the stylized two time slot system as a function of the VRE share μ. Results are presented for two different baseload capacities $\Gamma_{Base} = 2$ GW and 5 GW. The net storage impact $\Delta_\sigma e_{Base}$ on the baseload power plants' production as a function of μ is shown in the panels h and p: In general, it manifests itself as a storage-induced increase of production for small VRE shares, followed by the active storage-induced replacement (panel p). Throughout the rest of this paper, this pattern is a recurring result. While it is qualitatively independent of the storage and system parameters, the underlying mechanisms depend on the configuration details. This is explained below: For each of the two baseload capacity cases, the system interactions are discussed based on the constraint combinations which constitute the least cost solutions for the given parameter values.

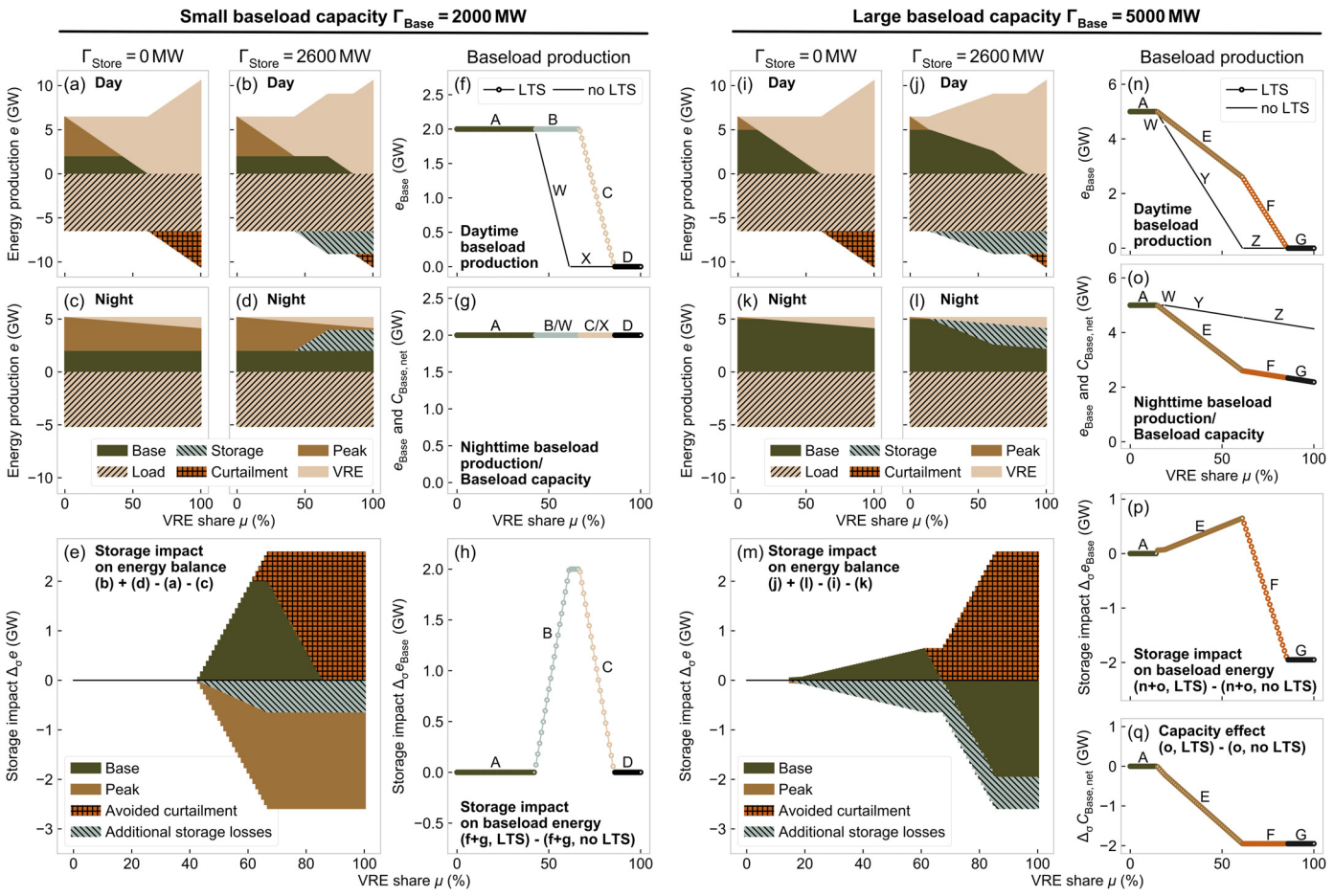

Fig. 6. Impact of long-term storage (LTS) in the stylized two time slot model for the extreme cases of low (Γ_{Base} = 2 GW, a-h) and high (Γ_{Base} = 5 GW, i-q) baseload capacity as a function of the VRE share μ. The storage power capacity Γ_{Store} is 0 or 2.6 GW. The dispatch during the two time slots is shown in the panels a-d (i-l); here, demand-like energy (load, charging, curtailment) is shown as negative values. The storage impact on the total energy balance is shown in panel e (m). The baseload production by constraint combination (see Table 5) is shown in the panels f-g (n-o). The panel h (p) shows the storage impact on net baseload power production by constraint combination. The baseload capacity (GW) is equal the night-time production (GWh/h) in all cases—panels g and o. In the C_{Base} = 2 GW case, the net installed capacity $C_{Base,net} = \Gamma_{Base} - C_{Base,ret}$ is not affected by storage; for C_{Base} = 5 GW the storage capacity effect (storage-induced impact on net capacity) is shown in panel q. VRE shares are varied in steps of 1%. The energy storage impact operator Δ_σ is defined in Section 2.2.

3.1.1.1. Low installed baseload capacity. The case of long-term storage and low Γ_{Base} = 2 GW is shown in the panels a–h. The labels in the panels f–h refer to the constraint combinations defined in Table 5. The storage impacts in these constraint combinations are the following:

A Storage idling: Production from peaker plants with identical variable costs causes the day-night marginal production cost difference to be zero. Therefore, storage is idling (panel e).

B Positive impact: Once VRE production is large enough to fully replace daytime peakload production (panel a), the energy transfer from day to night becomes a viable option. In the absence of storage, VRE replaces baseload power; therefore, storage allows baseload capacity to produce larger amounts of electricity during the day (panel b, also compare W and B in panel f). This additional production increases for larger VRE shares. The increasing net positive impact on baseload production is shown in panel h. Stored energy is then used to avoid production from peaker plants at night (panel d). As a result, the net impact of storage on baseload production is positive and growing as a function of μ. The positive impact stays constant once VRE production in the absence of storage fully replaces the baseload production during the day (constraint combination X, panel f). This happens at μ = 62%. Here, the baseload capacity constraint inhibits greater power production for charging. Additional charging power is covered with otherwise curtailed energy (small triangle above the baseload trapezoid in panel e).

C Decreasing positive impact: Storage operation is limited by the daytime charging power capacity and cannot absorb additional energy. For even higher VRE shares, storage is increasingly charged by otherwise curtailed power instead of additional baseload electricity (panel e). Consequently, the positive impact $\Delta_\sigma e_{Base}$ decreases (panel h).

D No impact: For large enough VRE shares, baseload production is fully avoided during the day (panel b). Only peakload production is replaced at night. Therefore, the storage impact on baseload $\Delta_\sigma e_{Base}$ is zero. However, if VRE production were increased even more, it would entirely replace the peaker production at night. Then, increasingly large shares of storage discharging power would be used to replace baseload production, resulting in $\Delta_\sigma e_{Base} < 0$ (not shown).

3.1.1.2. High installed baseload capacity Γ_{Base} = 5 GW. The large baseload capacity case is different in that peakload production at night is entirely replaced by a relatively small VRE share of 15% (panel k). Without peakload production, the storage impact is equally positive at first (panel p, constraint combination E), albeit for different reasons:

A Increasing positive impact: Under the constraint combination E, no power is produced from peaker plants. In this case, the retirement of baseload plants is the driving force behind storage operation: More baseload electricity is generated during the day to avoid the production during the night (compare panels o and n). Therefore—in this stylized case—the baseload production during the two time slots is exactly equal (panels j and l). Because of this, an increasing amount of capacity can be retired for greater VRE shares (panel q). The capacity factor is 100%. Note that the net baseload capacity $C_{\text{Base,net}} = \Gamma_{\text{Base}} - C_{\text{Base,ret}}$ is equal to the nighttime baseload production (panel o). This is because the night time power production $p_{\text{Base,night}}$ is always greater than or equal to $p_{\text{Base,day}}$, such that capacity retirements are limited by the former.

Baseload production is reduced during the night and increased during the day; storage's net positive impact $\Delta_\sigma e_{\text{Base}}$ (panel p) is the sole result of its limited round-trip efficiency (panel m): Additional baseload power production compensates the 25% energy losses between charging and discharging (Table 2). Perfectly lossless storage would not cause increased baseload production in this case.

B Decreasing positive impact/negative impact: Once the capacity limit of storage is reached, the replacement of baseload at night remains the same (panel o, identical slopes of F and Z), while increasing VRE production during the day reduces the baseload contributions to charging (panels j and n). This results in a continuous reduction of the positive net storage impact $\Delta_\sigma e_{\text{Base}}$, which finally turns negative (panel p).

C Constant negative impact: When daytime VRE production exceeds storage power capacity plus daytime demand, electricity is curtailed (panel j). Then, no additional storage-induced baseload replacement is possible and the negative storage impact $\Delta_\sigma e_{\text{Base}}$ stays at a constant negative level.

3.1.1.3. Intermediate installed baseload capacity $\Gamma_{Base} = 4.6$ GW. Fig. 7a–e shows the intermediate baseload capacity case $\Gamma_{\text{Base}} = 4.6$ GW for LTS. It constitutes a mix of the two cases with $\Gamma_{\text{Base}} = 2$ and 5 GW (Fig. 6)—both mechanisms of storage-induced baseload production increase are relevant:

- For smaller VRE shares μ the replacement of nighttime peakload production (constraint combination B, Fig. 7d);
- For larger μ the capacity utilization optimization and compensation of round-trip losses (constraint combination E, Fig. 7d).

Thereby, the transition is gradual: Between μ =23 and 56% (overlap of the constraint combinations E and W in Fig. 7b and c) decreasing volumes of peak power are replaced by storage discharging (panel a). This is because VRE replaces these generators already in the reference case without storage (W). Instead, larger amounts of charging power are covered by incremental daytime baseload production (note the increasing difference between E and W in panel 7b). Thereby, storage losses require additional daytime baseload production and therefore cause a net increase of e_{Base} (corresponding to the constraint combination E in Section 3.1.1). Once the peaker plant production is fully replaced by VRE in the reference case (Y and Z), the situation is identical to the high-Γ_{Base} case in Fig. 6.

3.1.1.4. The STS case. Fig. 7f–j shows the intermediate $\Gamma_{\text{Base}} = 4.6$ GW case for STS, i.e. short-term storage with higher round-trip efficiency $\eta = 90\%$. The net storage impact on baseload production (panel i) is qualitatively identical to the LTS case (panel d): An increase at low VRE shares μ is followed by the active storage-induced replacement $\Delta_\sigma e_{\text{Base}} < 0$ of baseload production. However, the amplitudes of both the negative and positive impacts are lower.

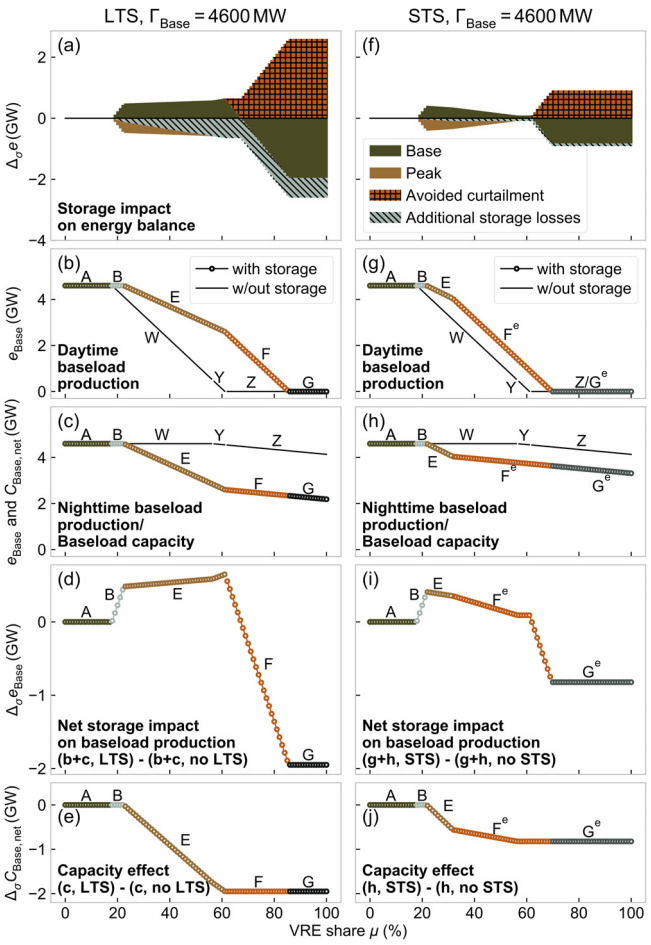

Fig. 7. Stylized two time slot model results; a/f: impact of 2.6 GW of long-term (LTS) and short-term storage (STS) on the total energy balance in the intermediate baseload capacity case ($\Gamma_{\text{Base}} = 4.6$ GW); b–c/g–h: the baseload production by constraint combination during both time slots; d/i net storage impact $\Delta_\sigma e_{\text{Base}}$ on baseload production; e/j: storage impact on baseload capacity $\Gamma_{\text{Base}} - C_{\text{Base,ret}}$. VRE shares are varied in steps of 1%. The energy storage impact operator Δ_σ is defined in Section 2.2.

This is due to both the higher round-trip efficiency of STS and the shorter discharge duration (lower energy capacity). Since the discharge duration (4 h) is smaller than the time slot duration (12 h), the charging power capacity constraint will never be active. Instead, the energy capacity is the limiting factor (constraint combinations with superscript "e", see Table 5).

The initial increase (constraint combination B) is identical to the LTS case and determined by the rising VRE share in both cases (compare panels d and i): Storage operation is unconstrained; the net baseload increase is only determined by the charging power, which is the same for LTS and STS.

As soon as the peaker plant production during the night is fully replaced by storage discharging, the capacity utilization optimization (E) starts to become more important. This means that gradually more nighttime baseload production is replaced, instead of nighttime peakload production. Unlike the LTS case, the lower losses of STS do not overcompensate this reduction of the nighttime baseload production. Because of this, the positive impact under the constraint combinations E and F^e gets gradually smaller. Storage with $\eta = 100\%$ would have zero net effect on baseload production in the capacity utilization optimization case. In addition, the low energy capacity of STS causes the constraint combination F^e (binding storage energy capacity constraint) to be reached for relatively small μ.

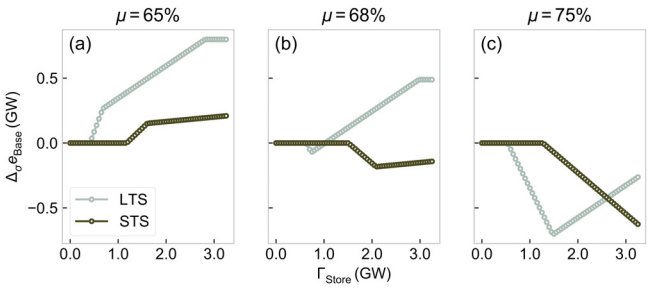

Fig. 8. Qualitatively diverging impact of the two different storage types at $\Gamma_{Base} = 4$ GW in the stylized two time slot model. For certain choices of the VRE share μ, the sign of the storage impact on baseload $\Delta_\sigma e_{Base}$ can be the opposite depending on the storage parameters. The storage capacity is varied in 50 MW steps. The energy storage impact operator Δ_σ is defined in Section 2.2.

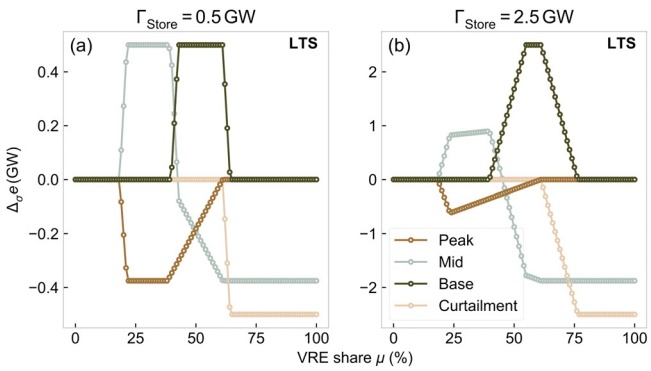

Fig. 9. Storage impact on the production from 3 power plants in the stylized two time slot model. With additional power plants in the system, storage enables a sequence of mutual replacements, ending with midload and baseload production being replaced by otherwise curtailed electricity. This shows the LTS case. VRE shares are varied in $\Delta\mu = 1\%$ steps. The energy storage impact operator Δ_σ is defined in Section 2.2.

The net positive storage impact on baseload reaches a constant level (independent of μ) when all nighttime peaker production is replaced by VRE even in the absence of storage capacity (constraint combination Y, Fig. 7i, g, and h). Then the storage impact is limited to pure capacity utilization optimization, within the tight STS energy capacity constraint.

Finally, the case where more and more charging is covered by otherwise curtailed daytime VRE production is identical to the LTS case (Figs. 7a–e and 6i–q). However, the lower energy capacity limits the negative impact $\Delta_\sigma e_{Base} < 0$.

3.1.2. Dependence on storage parameters

The transition from positive ($\Delta_\sigma e_{Base} > 0$) to negative storage impact on baseload production ($\Delta_\sigma e_{Base} < 0$) occurs for lower μ values in the STS case (Fig. 7i) as compared to the LTS case (Fig. 7d). Consequently, for certain VRE share ranges the two storage types have opposite effects on baseload production: STS contributes to its replacement ($\Delta_{\sigma_{STS}} e_{Base} < 0$), while LTS causes greater baseload production when compared to the no-storage reference case ($\Delta_{\sigma_{LTS}} e_{Base} > 0$).

Fig. 8 further illustrates how the qualitative storage impact can diverge for different storage types in the stylized two time slot model. Here, storage power capacity is varied for three selected VRE penetration levels. As in Figs. 6 and 7, higher VRE shares cause storage to have a negative net effect on baseload power production (Fig. 8c); for smaller μ it is the opposite (Fig. 8a). At $\Gamma_{Base} = 4$ GW a $\mu \in [67\%, 72\%]$range corresponds to the interesting narrow case where the two different storage types have opposite qualitative effects on net baseload power production. The $\mu = 68\%$ case is shown in panel b.

- **Short-term storage (STS)**: At $\mu = 68\%$, very small STS capacity is entirely charged from otherwise curtailed power during the day. The discharge replaces peaker plants at night. Because of this, the impact on baseload production is zero (Fig. 8b). Larger Γ_{Store} causes the complete replacement of nighttime peaker plant output. Consequently, additional storage capacity replaces the baseload. This explains the drop $\Delta_{\sigma \geqslant 1.5GW} e_{Base}$. For $\Delta_{\sigma \geqslant 2.1GW} e_{Base}$, the negative STS impact is partly compensated by daytime baseload charging (constraint combination F^e), since the storage capacity is large enough to absorb all curtailed energy. Through this baseload charging, large storage capacity erodes its own net negative impact.
- **Long-term storage (LTS)** equally causes a small reduction for low capacities (Fig. 8b). As in the STS case, this is due to charging from otherwise curtailed energy, and nighttime baseload replacement. However, the large storage energy capacity quickly reverses this trend: Compared to STS, much larger amounts of energy are absorbed during the day. This leads to the net positive impact $\Delta_{\sigma > 1GW} e_{Base} > 0$. In this case, the constraint combination F is active.

3.1.3. Multiple plants

The stylized two time slot model can be generalized by adding an additional power plant. This is shown in Fig. 9. In total, three plant types with flat cost supply curves are included in the system: Inexpensive baseload production and more expensive midload capacity, both with $\Gamma = 3.5$ GW, as well as unconstrained peaker plants.

This configuration illustrates the storage-induced sequential mutual replacement of different power plant types. For $\Gamma_{Store} = 0.5$ GW (panel a) the storage capacity is small relative to the installed power plant capacities and the VRE production; therefore, the mutual interactions are relatively clean: First, storage replaces peaker plants by discharging energy charged from midload plants, then baseload plants benefit from the replacement of midload and peaker plants. Finally, midload plants are replaced by stored energy which would otherwise have been curtailed. The replacement of baseload is not included in Fig. 9 and would occur for even higher μ.

For larger Γ_{Store} (panel b), the limiting factor is not the storage power capacity (as for $\Gamma_{Store} = 0.5$ GW in panel a), but the VRE share: Greater μ gradually provide additional replacement opportunities. Because of this, the storage impact $\Delta_\sigma e$ increases for larger μ until storage operation is capacity constrained. This occurs at $\mu = 22$ and 44% in panels a and b, respectively.

3.2. Quadratic dispatch model

This section demonstrates that the basic patterns found for the stylized model with two time slots also apply to the more complex case of the quadratic dispatch model with hourly resolution (model description in Section 2.1).

While five countries are included in the dispatch model, this analysis focuses on a subset: France with its predominantly nuclear power generation portfolio (RTE, 2016) provides a clean case of baseload capacity replacement; Germany's coal and nuclear centered yet overall diverse power system (BMWi, 2016) illustrates the sequential storage-induced mutual replacement of power plant types.

3.2.1. Impact on nuclear power indicators

Interaction with nuclear power plants is a prime example of storage impact: Due to their low variable cost, these plants operate at the top of the merit order. Therefore, their interaction with VRE and storage is comparatively isolated from other system compo-

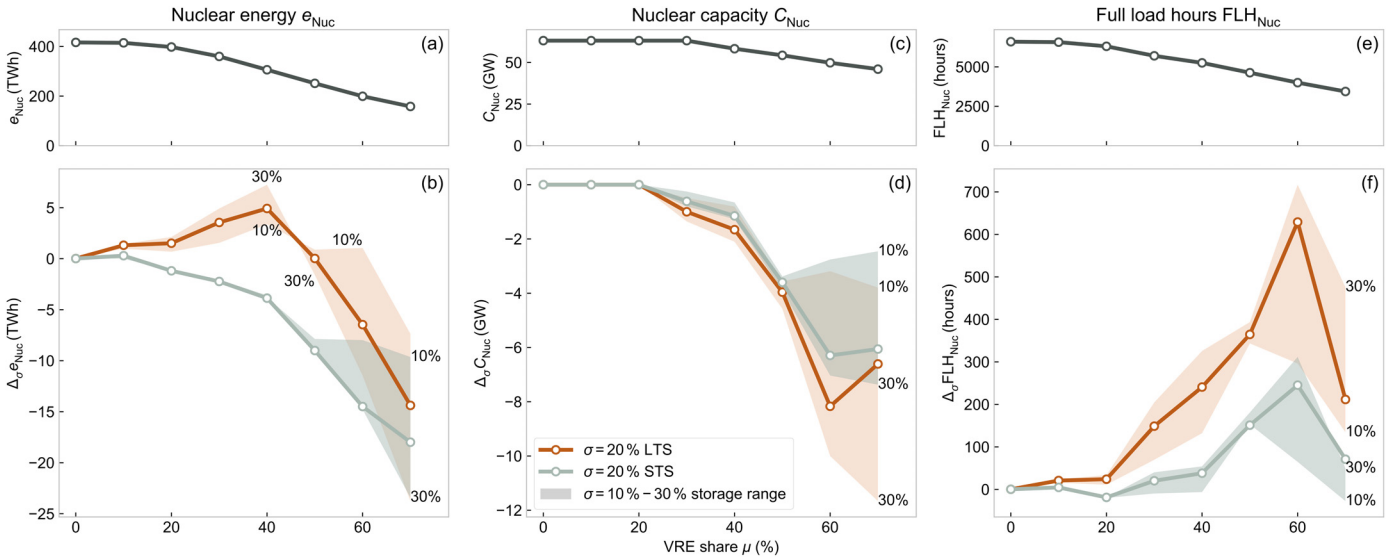

Fig. 10. Dispatch model results; panels a, c, e: impact of VRE on nuclear power production, capacity and full-load hours in France in the absence of additional storage as a function of μ; panels b, d, f: storage impact on the same indicators. The storage impact operator Δ_σ is defined in Section 2.2. VRE shares are varied in $\Delta\mu = 10\%$ steps.

nents. This allows for a good comparison with the two power plant case of the stylized model (Section 3.1.1). Fig. 10 shows the storage impact on various nuclear power indicators in France:

- Without storage, the electric energy production e_{Nuc} experiences a near-linear replacement for VRE shares $\mu \geqslant 20\%$ (panel a). In the presence of 20% LTS, this replacement is compensated by additional nuclear energy production up to a maximum of nearly $\Delta_{\sigma=20\%} e_{Nuc} = +5$ TWh or +1.6% at a VRE share $\mu = 40\%$ (panel b). This pattern is in agreement with the stylized model results (Fig. 6). For STS, additional demand due to storage round-trip losses is reduced, and the smaller energy capacity limits the storage operation. Because of this, the net effect $\Delta_\sigma e_{Nuc}$ is zero or negative for all μ and σ. The positive impact of LTS grows near-linearly as a function of storage capacity σ for $10\% \leqslant \sigma \leqslant 30\%$. In contrast, the impact of STS is fully saturated for $\mu \leqslant 50\%$ and $\sigma \geqslant 10\%$, such that the exact storage capacity value has very little impact ($\Delta_{\sigma_{STS}=10\%} e_{Nuc}(\mu = 40\%) \approx \Delta_{\sigma_{STS}=30\%} e_{Nuc}(\mu = 40\%)$).

  Positive storage impact followed by negative impact also corresponds to a delay of the VRE-induced replacement of nuclear power: In the presence of LTS, higher μ are required to replace nuclear power with VRE (compared to the no-storage case in panel a), but—for even higher VRE shares—the VRE-induced replacement occurs more quickly and is ultimately stronger.
- The installed capacity $C_{Nuc,net} = \Gamma_{Nuc} - C_{Nuc,ret}$ (panels c, d) is reduced by storage for all $\mu \geqslant 30\%$. This is qualitatively identical to the toy model, where storage capacity is used to avoid fixed O&M costs by spreading out the VRE-induced baseload replacement across the time slots (Fig. 6q, capacity combination E). Since the storage penetration σ is defined in terms of power capacity, the two storage types have very similar impact on nuclear capacity: A given power capacity of both LTS and STS can replace the same amount of nuclear capacity. It is only for the largest VRE shares $\mu \geqslant 60\%$ that the specific storage properties make a difference. Also in the stylized model, the replacement of baseload capacity is very similar for STS and LTS at small VRE shares μ (constraint combination E in Fig. 7e and j).
- The storage impact on energy and capacity allows for major capacity utilization increases (panels e and f in Fig. 10). In the presence of less efficient LTS, the maximum impact on full-load hours (FLH) amounts to $\Delta_{\sigma=20\%} FLH = 630$ h (+ 15.7%). This is the case at a high VRE penetration of $\mu = 60\%$. A prerequisite for this FLH increase is the low utilization in the reference case without additional storage: Nuclear power plants produce only 4000 full load hours, as compared to nearly 6600 for $\mu = 0\%$ (panel e).

  The impacts of LTS and STS are qualitatively identical, but the former is more pronounced: This is both due to smaller energy replacement for LTS (panel b) as well as greater capacity retirement (panel d). In the 20% STS case, the maximum increase at $\mu = 60\%$ amounts to 245 h (+ 6.1%).

  It is important to note that the impact on full load hours is generally positive and substantial: Bulk storage replaces the least efficient plants and allows the rest to operate under optimized conditions, i.e. with higher capacity factors. However, part of these improved conditions is caused by storage round-trip losses and hence a decrease of total system energy efficiency. This is similarly the case for all other dispatchable power plant types in all countries (see the table in the supplementary material, section B). Thereby, storage impact on FLHs is generally positive even when the impact on power production is negative. This means that the negative impact on *capacity* is even stronger.

Fig. 11 provides additional insights into the system changes associated with the storage impact on nuclear power in France:

- In the *LTS* case (panel a) positive storage impact on nuclear goes hand in hand with increased curtailment avoidance, an increase of exports, and—to a lesser degree—the decrease of imports. Fossil generators (not displayed) play only a minor role in the French power supply and are barely affected in terms of absolute volumes. In addition to interactions with foreign generation, round-trip losses of new storage capacity are a net driver of additional electricity production. This is partly compensated by the reduction of incumbent PHS operation. For larger VRE shares μ, nuclear power is primarily replaced due to charging from otherwise curtailed electricity.
- As shown in Fig. 10, *STS* impact $\Delta_{\sigma=20\%} e_{Nuc}$ is consistently negative (Fig. 11b). Storage replaces nuclear power predominantly by charging otherwise curtailed energy. The additional demand due to storage round-trip losses is much smaller when compared to LTS.

The dispatch model results are generally in agreement with the discussion based on the stylized model (Fig. 7d and i). An inter-

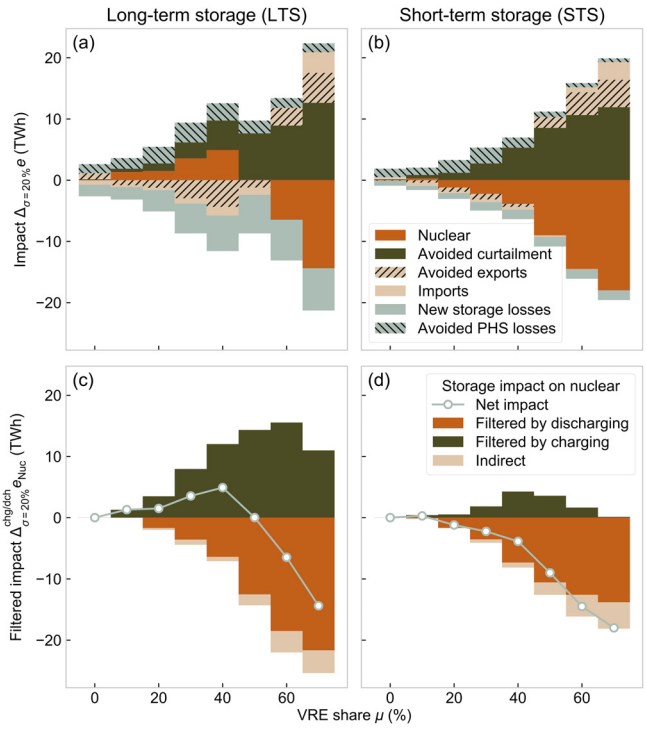

Fig. 11. Panels a–b: System changes in France due to $\sigma = 20\%$ storage additions in the dispatch model. These data represent differences in energy balances and sum up to zero. The *Nuclear* power data series correspond to the $\sigma = 20\%$ series in Fig. 10b. Panels c–d: Change in nuclear power output filtered by storage charging and discharging. The *Net impact* series corresponds to the *Nuclear* data in a and b. *Discharging* is exclusively associated with a *reduction* of nuclear power, *charging* with an *increase*. The storage impact operator Δ_σ is defined in Section 2.2. VRE shares are varied in $\Delta\mu = 10\%$ steps.

esting discrepancy is the lack of positive STS impact in Fig. 10b. This can be explained by considering the storage impact on the total energy balance in Fig. 11b: In the dispatch model, storage causes the absorption of otherwise curtailed energy already for the smallest μ. This is in contrast to the stylized model (Fig. 7f), where charging from otherwise curtailed energy only becomes relevant for much higher VRE shares. In addition, losses from the operation of incumbent PHS plants are reduced due to the switch to efficient batteries. This also contributes to the stronger nuclear power replacement.

3.2.2. Simultaneous positive and negative impact

Storage impact on power production is generally the net combination of simultaneous positive and negative effects during a given year. In the stylized model, this is the case for the constraint combination E, where storage charges baseload production during the day, to replace power generation from the same plants at night. As discussed in Section 3.1.1, this allows for cost reductions due to capacity retirements.

This also holds in the case of the more complex dispatch model. Here, also seasonal effects can play a role. These are not captured by the stylized model. For example, the reduced nuclear capacity availability during summer causes imbalances between the seasons and therefore potentially qualitatively diverging storage impact during different months of the same year. The seasonality of the PV and wind power resource availability has the same effect.

To analyze these counteracting contributions, the subsets of hours $\mathcal{H}_{chg} \subset \mathcal{H}$ and $\mathcal{H}_{dch} \subset \mathcal{H}$ are defined, during which additional storage is charging or discharging, respectively: $\mathcal{H}_{chg/dch} = \{t \in \mathcal{H} | p_{chg/dch,t} > 0\}$. The storage impact on nuclear power is then considered separately for these subsets:

$$\Delta^{i}_{\sigma=20\%} e_{Nuc} = \sum_{t \in \mathcal{H}_i} \left(p^{\sigma=20\%}_{Nuc,t} - p^{\sigma=0\%}_{Nuc,t} \right), \quad i \in \{chg, dch\}. \tag{10}$$

These two quantities are plotted in Fig. 11c and d:

- *Discharging* is exclusively associated with a *reduction* of nuclear power, *charging* with an *increase*. This finding is in line with expectations and corresponds to the results of the stylized model (positive impact during the day, negative or zero impact at night—Fig. 6). However, its consistency in the dispatch model is surprising, given the complexity of the system. In the Swiss case, where nuclear power has a much smaller capacity share and is replaced for high μ only, a certain degree of mixing occurs due to interactions with other system components (not shown).
- The sum of the charging and discharging impact is only an approximation of the total net storage impact: In general, storage may affect nuclear power production also during hours where it is idling. This can happen for two distinct reasons: (i) Capacity effect: If storage operation results in nuclear capacity retirements (analogous to the stylized model, Section 3.1.1), nuclear power production during *all* hours is affected. (ii) Energy effect: Storage discharging might avoid the production from hydro reservoir plants. Then a certain amount of energy is freed up for use during other time slots, where it might replace nuclear power production (indirect impact due to relaxed energy constraints).

  Fig. 11c and d show these indirect impacts as separate data series. They are generally negative.
- The filtered positive and negative storage impacts can be significant even if the yearly total sums up to zero. This is the case for $\mu = 50\%$ in the presence of LTS (panel c): During charging hours, nuclear output increases by 14.3 TWh (+ 5.7% of total nuclear production), during discharging hours it is reduced by 12.5 TWh (− 5.0%, without *indirect* contributions). The total net storage impact is negligible at less than 0.1%. In the stylized model this can equally be observed (Fig. 6): Here the net impact at $\mu = 67\%$ is negligible (panel p), while the positive impact during the day (panel n), and the negative impact at night (panel o) are both substantial.
- While STS causes net replacement of baseload for virtually all VRE shares μ, it does lead to greater production during charging hours for certain μ (panel d). This positive impact is entirely hidden in the aggregate analysis (panel b).

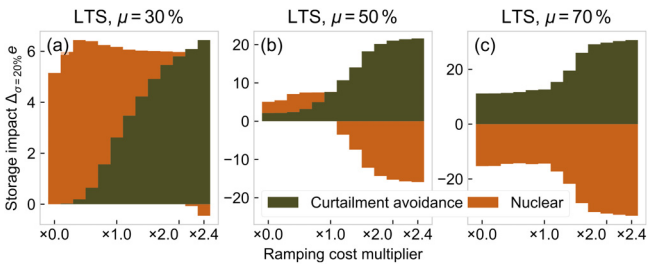

Fig. 12. Dependence of the storage impact on the ramping cost in the dispatch model's French LTS case. All default ramping costs are varied by multipliers between ×0.0 and ×2.4 in steps of 0.2. The storage impact operator Δ_σ is defined in Section 2.2.

3.2.3. Ramping cost sensitivity

As discussed in the methods section, ramping costs are modeled as variable costs on hourly generator output changes. In Fig. 12 the original cost assumptions are varied over a range (×0.0−×2.4) for three different VRE shares. This is shown for the case of French nuclear power.

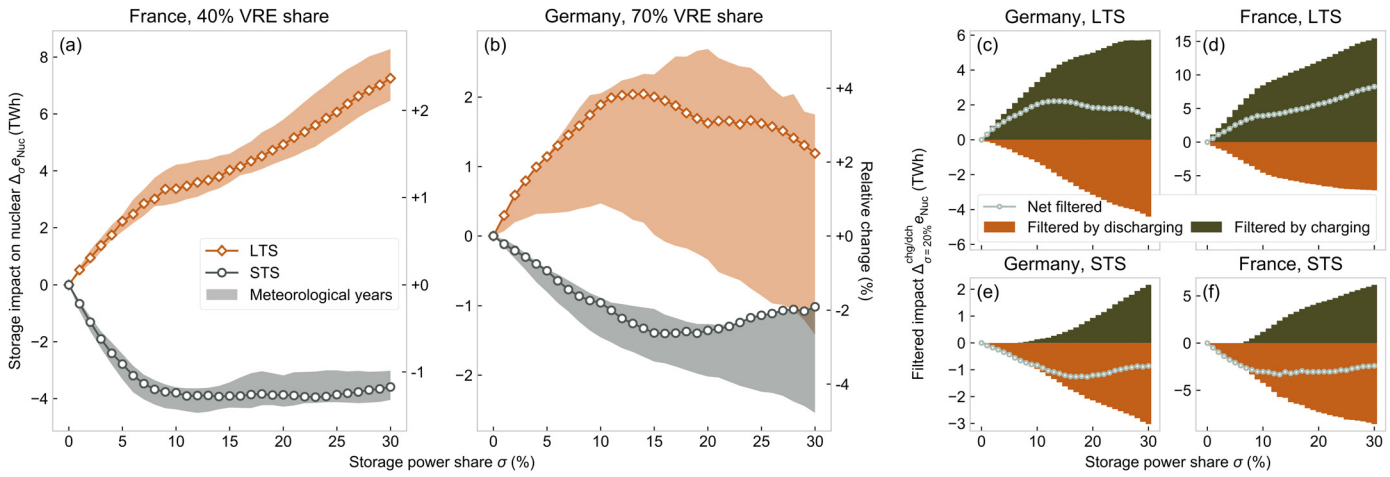

Fig. 13. Difference in electricity production $\Delta_\sigma e_{Nuc}$ from nuclear power in France (a) and Germany (b) as a function of the storage power share σ (varied in 1% steps) in the dispatch model. The $\sigma = 20\%$ data points in France correspond to the $\mu = 40\%$ data points in Fig. 10b. The data shown in the panels c-f results from the same filtered analysis as described in Section 3.2.2 for the default year 2015. The energy storage impact operator Δ_σ is defined in Section 2.2.

Without additional storage, higher ramping costs consistently lead to increased nuclear power output (not shown). This is caused by the penalties of adapting the production to the VRE profile: It is beneficial to operate plants at a higher constant level.

Consequently, storage impact changes as a function of $c_{ramp,pp}$: In general, higher cost leads to smaller positive or larger negative storage impact on nuclear power production. This can be understood as follows:

1. In the absence of storage, nuclear power production is elevated due to expensive ramping.
2. In the absence of storage also curtailment is higher for greater ramping costs. This happens when the cost of power output reduction outweighs the costs of overproduction.
3. Therefore, higher ramping costs cause storage to be charged from otherwise curtailed energy to a greater extent. This charged energy is then used to replace nuclear power or to induce other system changes. This trend can be seen for all VRE shares in Fig. 12.

An interesting example is given by the $\mu = 30\%$ LTS case (Fig. 12a): The total storage impact on nuclear power production and curtailment reduction is roughly constant. However, the nuclear power contribution decreases from 100% to zero as the ramping cost is changed from zero to double the default.

3.2.4. Qualitatively diverging impact of storage types

Using the stylized model it was shown that different storage types can have qualitatively diverging impact on the production from certain plants (see Section 3.1.2, Fig. 8). This is because the standard storage impact pattern as a function of the VRE share μ (positive followed by negative impact) is delayed for LTS with large energy capacity and low efficiency. Therefore, μ-ranges exist where the storage impact sign is the opposite depending on which of the storage types is added to the system: LTS causes the increase of nuclear power production, while STS causes its decrease. For the dispatch model, this is shown in Fig. 13 for two of the modeled countries which make use of nuclear power production. For this illustration, the VRE share μ with the cleanest separation is selected (out of multiples of 10%). In France, where nominal installed nuclear capacity amounts to 116% of average demand (RTE, 2016), even small VRE production volumes have a noticeable impact on this technology. Therefore, the divergent behavior occurs already for $\mu = 40\%$ (panel a). On the other extreme, the installed nuclear capacity is approximately 17% of average load in Germany (BMWi, 2018), and its output is replaced only for the highest considered VRE share $\mu = 70\%$.

In the German case, the impact of storage is much more sensitive with respect to the parameter configuration. In Fig. 13a–b this is illustrated by the shaded areas, which represent the dependence on the wind and solar profile shape (see method Section 2.1.2). In France, the VRE profile selection does not affect the storage impact to any significant degree. This is because of the nuclear power predominance, which makes this interaction robust: For $\sigma = 20\%$, the storage impact on French nuclear power production amounts to 54.1% (38.2%) of the total negative (positive) storage impact (compare Fig. 11 a–b). In contrast, these values are much smaller in Germany (12.4% and 6.7%, respectively): In the German case, storage is simultaneously used to optimize the operation of hard coal and lignite fueled power plants (Section 3.2.5).

In addition to this parameter dependency, the small German nuclear power production shares also cause distinct minima (maxima) of the negative (positive) storage impact (Fig. 8b, at around $\sigma = 15\%$). This is because larger σ enable additional counteracting mechanisms: Larger storage capacity self-compensates its impacts, e.g. negative impacts are partly compensated by positive impacts during different hours. The stylized model case (Fig. 8b) is equivalent: There, STS capacities Γ_{Store} beyond 2.1 GW cause a reduction of the negative impact. The underlying reason is the absorption of all otherwise curtailed energy by large enough storage capacities. Then, even larger Γ_{Store} charges increasing amounts of energy from additional daytime baseload production. In the dispatch model, the situation is very similar: German short term storage first replaces nuclear power before gradually causing more output from the same plants during the charging hours (Fig. 13e). This explains the STS curve's minimum in panel b. Fig. 13c shows that the net reduction of $\Delta_\sigma e_{Nuc} > 0$ can be attributed to a saturation of the positive impact: For large enough σ, the opportunities for additional baseload production are fully exploited.

In France, no distinct minima and maxima are observed in Fig. 13a—only the negative STS impact saturates. Again, this is attributed to predominance of this power plant technology.

3.2.5. Sequential replacement

Using a stylized model with multiple power plant types (Section 3.1.3), it can be shown that larger VRE volumes replace assets which operate increasingly high in the merit order. Consequently, the storage impact changes with μ: Power plant types which ben-

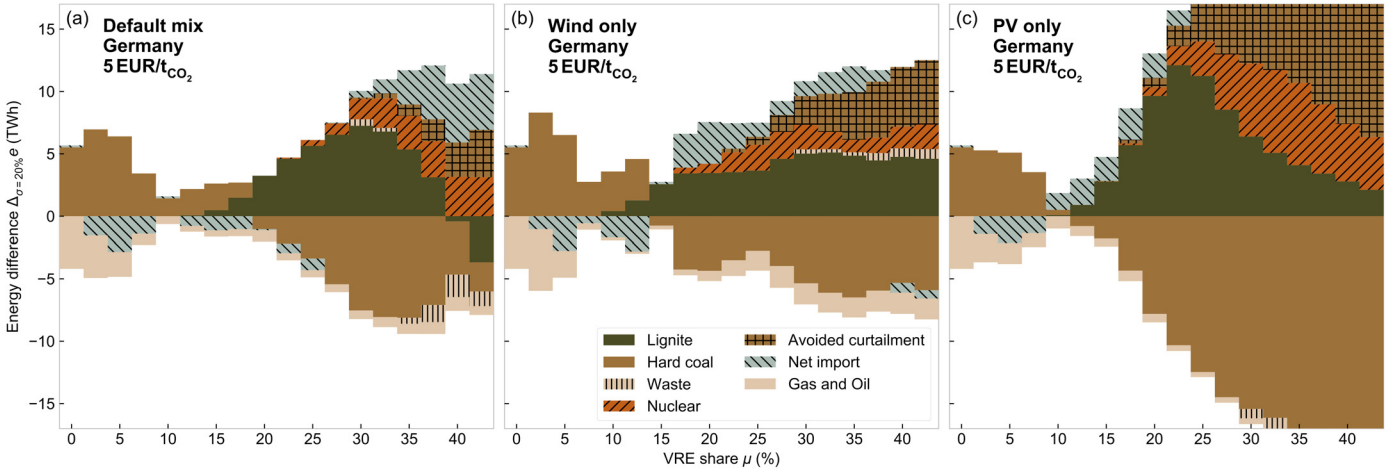

Fig. 14. LTS-induced energy balance differences $\Delta_{\sigma=20\%}e$ in Germany (dispatch model). VRE shares μ are varied in 2.5% steps. The storage impact operator Δ_σ is defined in Section 2.2.

efit from storage at lower VRE shares μ are actively replaced at higher μ; power plants previously unaffected by VRE and storage experience an impact. This results in a sequence of mutual replacements.

The German example in the quadratic dispatch model is shown in Fig. 14 for $\sigma = 20\%$. The panels a–c contrast the default VRE mix (Fig. 3) and the pure wind and solar profiles. Note that the German low-μ cases are purely hypothetical and only serve the exploratory character of this study: The country's 2015 gross wind and solar power production share amounted to 18.2% (German Federal Ministry for Economic Affairs and Energy (BMWi), 2018).

3.2.5.1. Impact of the VRE mix. For the default VRE mix (panel a) and the pure PV profile (b), a distinct minimum of the cumulative storage impact $\sum_{pp}\Delta_\sigma e_{pp}$(TWh) is reached for $\mu = 10\%$: For small μ, the impact of solar power production consists of a reduction of the daily demand peak. Because of this, the storage impact is reduced. To some extent, the case of wind power is similar: Also here the VRE profile will first reduce the demand for peaker plants during certain days, before shaping the profile itself and increasing the potential for energy time-shifting. However, the wind profile is less correlated with the daily demand shape, which mitigates this effect.

The storage impact minimum corresponds to the findings of Hartner and Permoser (2018): For the German case they identified a minimum of storage revenues in Germany as a function of the PV share at roughly 5% of total electricity generation. Their study identifies the daily demand peak erosion due to growing solar power production as the underlying cause.

For very high VRE shares, the maximum absolute storage impact in Germany is greatest for pure PV (32.8 TWh at $\mu = 42.5\%$) and smallest for a pure wind profile (12.1 TWh at $\mu = 37.5\%$). This is caused by the low capacity factor of the PV profile and its strong concentration within few hours at noon: Even comparatively small PV shares lead to significant curtailment.

In addition to these quantitative differences, the strict periodicity of the PV production results in smoother changes of the storage impact as a function of μ. For example, it eliminates the local maxima of storage impact on hard coal and nuclear in the case of pure wind power profiles (Fig. 14b),

3.2.5.2. Sequential replacement of generators. Concerning the mutual replacement of generators, storage has qualitatively almost identical impact for all three considered VRE profiles in Fig. 14: First, it causes the replacement of natural gas and net imports with hard coal. For the pure wind (b) and PV (c) profiles, this is the case up to around $\mu = 10$-12.5%. For the default mix (a), significant positive impact on hard-coal power production ends at a higher $\mu = 17.5\%$.

Beyond these VRE shares, the storage-induced replacement of hard coal is associated with an increase of cheaper lignite power production. For the default mix (a), lignite power is actively replaced by storage for $\mu > 37.5\%$.

Nuclear power is only affected at high VRE shares μ in Germany, independent of the parameter configuration. Up to $\mu = 70\%$, $\Delta_\sigma e_{Nuc}$ is always positive. The onset of $\Delta_{\sigma=20\%}e_{Nuc} > 0$ happens for $\mu = 22.5\%$ for the default VRE mix (panel a). In the cases of both pure wind (b) and pure PV (c) the impact starts at lower values ($\mu = 17.5\%$).

Curtailment avoidance makes much stronger contributions in case of the pure VRE profiles (b–c): The more balanced mixed default VRE profile (panel a) is less prone to cause power overproduction for any given μ.

Imports and exports play a pronounced role. Note that the relative economic competitiveness of cross-border transmission depends on the state of the system in all the neighboring countries. This makes the interaction highly complex. However, the qualitative and key quantitative results (onset and sign of storage impact on domestic generators) remain the same if the cross-border exchange is suppressed (not shown).

3.2.6. CO_2 price and emissions

The mutual replacements in Fig. 14 feature the avoidance of natural gas due to increases of hard coal fueled power production. For higher μ, storage causes the replacement of hard coal with lignite. Due to the carbon intensity differences of these fuels, the total domestic emissions E (Mt_{CO_2}) are also affected by storage. Fig. 15 shows the storage impact $\Delta_{\sigma=20\%}E$ (Mt_{CO_2}) by fuel and as absolute and relative totals for three different CO_2 prices. In line with the literature, certain threshold wind and solar shares are required to make the net storage operation carbon-neutral (Goteti et al., 2017).

In the 5 EUR/t case, both the storage-induced replacement of gas with hard coal and the replacement of hard coal with lignite power lead to net emission increases. For LTS, this gives rise to two distinct peaks as a function of the VRE share μ (panel a): At $\mu = 5\%$ domestic emissions increase by 5.6 Mt_{CO_2} (+ 1.5% relative to the no-storage case); for $\mu = 25\%$ emissions increase by + 3.7 Mt_{CO_2} (+ 1.7%).

The sequence of mutual replacements discussed in Section 3.2.5 is strongly influenced by the relative variable costs of power production. This cost is partly determined by the CO_2 emission price. In Germany, the individual cost supply curves of the considered plants are strongly overlapping at the 40 EUR/t_{CO_2} price level (see Fig. 2).

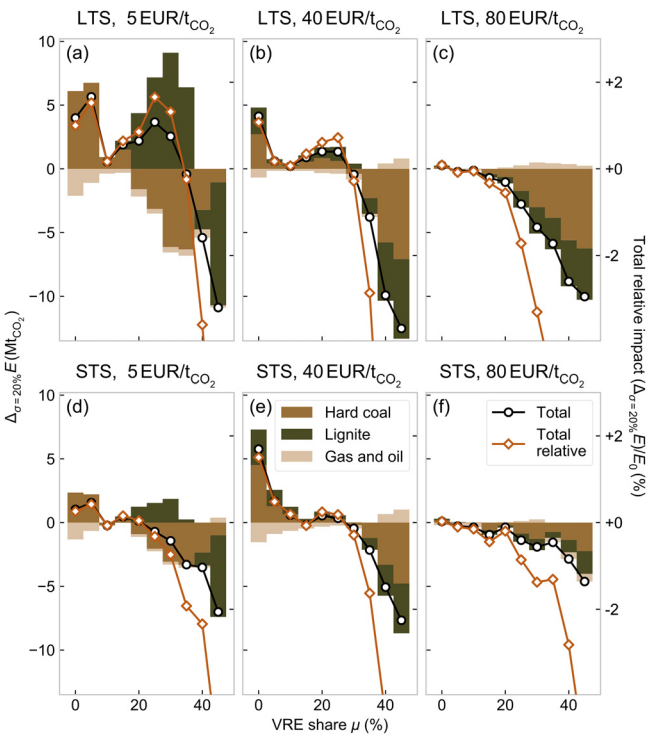

Fig. 15. Impact of storage on domestic emissions in Germany (dispatch model). The *Total relative* is the relative share of total domestic emissions and corresponds to the y-axis on the right. VRE shares μ are varied in 5% steps. The storage impact operator Δ_σ is defined in Section 2.2.

Therefore, the storage-induced mutual replacements of power production for increasing μ follow a less strict order when compared to the 5 EUR/t$_{CO_2}$ case (compare panels a and b in Fig. 15): Natural gas is initially replaced by hard coal and lignite (Fig. 15b). For greater μ, storage causes the joint replacement of hard coal and lignite with nuclear power and imports (not shown). Gas experiences storage-induced output *increases* for $\mu \gtrsim 40\%$, despite being replaced by storage at low VRE shares. These high-μ increases of gas fueled power production can equally be attributed to the supply cost structure (see the 40 EUR/t$_{CO_2}$ case in Fig. 2): Using the stylized modeling framework, it can be shown that overlapping linear cost supply curves of two plant types can give rise to this behavior (see supplementary material, section A).

Interestingly, for small μ in the 40 EUR/t$_{CO_2}$ case, more efficient STS (panel e) increases the net emissions more strongly than LTS (panel b). In this μ-range, marginal power cost differences tend to be too small to be exploited by LTS. This is due to the limited round-trip efficiency of this storage type. STS with $\eta = 90\%$ is therefore more active.

At 80 EUR/t$_{CO_2}$ and $\mu > 0\%$, storage has almost no positive net impact on emissions (Fig. 15c and f).

4. Limitations

The dispatch model itself is designed to capture many of the complexities of the real market situation. It is therefore well-suited to test the predictions of the stylized model in a more complex setting. Still, it remains a stylized approximation itself. The potential to draw policy recommendations applicable to current power systems is limited. However, the analysis highlights the necessity to understand the implications of profound system changes—like greater storage volumes—in a free market environment.

Some neglected aspects have the potential to impact the interaction between VRE, storage, and dispatchable generators. They could serve as starting points for future research:

- *Stronger coupling of the heat and electricity sectors* offers ample potential for the integration of VRE into the energy system (International Energy Agency, 2014): For example, it can increase the system flexibility by enabling the absorption of excess VRE production. At the same time, heat storage in an integrated energy system might provide similar services as bulk electric storage in a pure power system. This could offset the impact of additional electric storage. This coupling might become increasingly relevant for scenarios with higher VRE shares.
- *Origin of supply policies*—which limit the charging power to renewable power production—can be expected to lower the positive storage impact on conventional generator output. This also includes the mandated installation of storage capacity in support of renewable energy projects (REN21, 2018).
- *Taxes and levies on charged energy* would reduce the number of charging/discharging opportunities by adding an offset to the required price differential: For example, with τ the taxes per unit of charged energy, discharging electricity prices $\pi_{t_{\text{dch}}}$ would need to be greater than $(\pi_{t_{\text{chg}}} + \tau)/\eta$ for the energy time-shifting operation to be viable. Subsidies on charging energy would have the opposite effect.
- *Vertical network constraints and tariff structures* reduce the interaction of storage with the wholesale market, e.g. if storage is installed behind the meter in combination with residential PV systems. In this case, tariff and incentive structures influence storage operation (Pena-Bello et al., 2017) and hence its impact on assets connected to higher voltage grid levels.
- *Ancillary system services* provided by storage also affect storage-generator interactions (Nyamdash and Denny, 2013). Including these services in the model would add significant complexities to the dispatch: Generator capacity could be freed up if storage provides reserve capacity in its stead. At the same time, part of the storage capacity would not be available for the wholesale electricity markets.
- *Limitation to single storage technologies:* Considering only isolated storage technologies serves the purpose of investigating the storage parameters' influence. However, in most national size power systems, a balanced technology mix would be more realistic and superior in performance. This mix can be expected to have more pronounced impacts when compared to pure storage technologies.

5. Conclusion

In a free-market energy future based on the extensive interconnectedness of all consumers and producers, the impact of system changes requires careful evaluation to avoid unintended interactions. Large storage volumes can have substantial impacts on the operation of dispatchable electricity generating assets and influence whether or not they are replaced by variable renewable electricity sources (VRE). Policy designs in support of storage should be preceded by the detailed evaluation of storage's interaction with the energy system both in its status quo and considering its anticipated future development.

This study is centered on the storage impact in power systems with systematic parameter variations. Dispatchable power replacements in a system with large amounts of storage capacity are analyzed for increasing VRE penetrations. The primary goal is the discussion of the underlying interaction mechanisms between VRE, storage, and dispatchable plants in different settings. For this purpose, two complementary modeling frameworks are employed:

A dispatch model with quadratic cost objective and hourly resolution over a full year, which represents the operation and retirement of aggregated power plants in five European countries. In addition, stylized models are used to explain the market mechanisms of interest. They consist of the minimum number of system components required to explain the market mechanisms of interest, i.e. two time slots and two to three dispatchable power plant types.

Storage impact on the output of a given generator type as a function of the VRE share generally follows a characteristic pattern: At low VRE shares, the impact is positive, i.e. energy storage compensates the VRE-induced replacement of dispatchable production (e.g. nuclear or coal-based electricity); at high VRE shares, storage contributes to the replacement of the very same assets. The positive impact is found to be caused by (i) additional charging to replace generators lower in the merit order, (ii) capacity utilization optimization which requires additional power production to compensate for storage round trip losses. This basic pattern consistently arises in the more complex dispatch model. The stylized modeling framework with just two time slots and two generators allows for a fundamental discussion of the underlying principles.

This study lays the theoretical foundation for a more detailed assessment of the role of storage in the transitioning power system. Future work will focus on the integration of low-temperature heat and a detailed representation of the consumer side. These expansions will enable concrete policy recommendations.

Acknowledgments

The authors thank the anonymous reviewers for their excellent comments. This research is financially supported by the Swiss Innovation Agency Innosuisse and is part of the Swiss Competence Center for Energy Research in Heat and Electricity Storage (SCCER HaE) as well as the Competence Center for Research in Energy, Society and Transition (SCCER-CREST). It is also part of the project "The role of energy storage in the context of the Swiss energy transition" (acronym: SwissStore) funded by the Swiss National Science Foundation (SNF), grant number 205121_172703/1.

Appendix A. Supplementary data

Supplementary data to this article can be found online at https://doi.org/10.1016/j.eneco.2019.104495.

References

Babrowski, S., Jochem, P., Fichtner, W., 2016. Electricity storage systems in the future German energy sector: an optimization of the German electricity generation system until 2040 considering grid restrictions. Comput. Oper. Res. 66, 228–240, http://dx.doi.org/10.1016/j.cor.2015.01.014.

Brouwer, A.S., van den Broek, M., Zappa, W., Turkenburg, W.C., Faaij, A., 2016. Least-cost options for integrating intermittent renewables in low-carbon power systems. Appl. Energy 161, 48–74, http://dx.doi.org/10.1016/j.apenergy.2015.09.090.

Bussar, C., Stöcker, P., Cai, Z., Moraes Jr., L., Magnor, D., Wiernes, P., Bracht, N. v., Moser, A., Sauer, D.U., 2016. Large-scale integration of renewable energies and impact on storage demand in a European renewable power system of 2050-Sensitivity study. J. Energy Storage 6, 1–10, http://dx.doi.org/10.1016/j.est.2016.02.004.

Capros, P., Vita, A.D., Tasios, N., Siskos, P., Kannavou, M., Petropoulos, A., Evangelopoulou, S., Zampara, M., Papadopoulos, D., Nakos, C., Paroussos, L., Fragiadakis, K., Tsani, S., Karkatsoulis, P., Fragkos, P., Kouvaritakis, N., Isaksson, L.H., Winiwarter, W., Purohit, P., Sanabria, A.G., Frank, S., Forsell, N., Gusti, M., Havlik, P., Obersteiner, M., Witzke, H., Kesting, M., 2016. EU Reference Scenario 2016 - Energy, transport and GHG emissions Trends to 2050 (July) https://web.archive.org/web/20171026064411/https://ec.europa.eu/energy/sites/ener/files/documents/AppendixRefSce.xls.

Cebulla, F., Haas, J., Eichman, J., Nowak, W., Mancarella, P., 2018. How much electrical energy storage do we need? A synthesis for the U.S., Europe, and Germany. J. Clean. Prod. 181, 449–459, http://dx.doi.org/10.1016/j.jclepro.2018.01.144.

Creutzig, F., Agoston, P., Goldschmidt, J.C., Luderer, G., Nemet, G., Pietzcker, R.C., 2017. The underestimated potential of solar energy to mitigate climate change. Nat. Energy 2, 17140, http://dx.doi.org/10.1038/nenergy.2017.140.

de Boer, Sytze, H., Grond, L., Moll, H., Benders, R., 2014. The application of power-to-gas, pumped hydro storage and compressed air energy storage in an electricity system at different wind power penetration levels. Energy 72, 360–370, http://dx.doi.org/10.1016/j.energy.2014.05.047.

de Sisternes, Fernando, J., Jenkins, J.D., Botterud, A., 2016. The value of energy storage in decarbonizing the electricity sector. Appl. Energy 175, 368–379, http://dx.doi.org/10.1016/j.apenergy.2016.05.014.

Denholm, P., Hand, M., 2011. Grid flexibility and storage required to achieve very high penetration of variable renewable electricity. Energy Policy 39 (3), 1817–1830, http://dx.doi.org/10.1016/j.enpol.2011.01.019.

Després, J., Mima, S., Kitous, A., Criqui, P., Hadjsaid, N., Noirot, I., 2017. Storage as a flexibility option in power systems with high shares of variable renewable energy sources: a POLES-based analysis. Energy Econ. 64, 638–650, http://dx.doi.org/10.1016/j.eneco.2016.03.006.

Egerer, J., Gerbaulet, C., Ihlenburg, R., Kunz, F., Reinhard, B., von Hirschhausen, C., Weber, A., Weibezahn, J., 2014. Electricity Sector Data for Policy-Relevant Modeling. DIW, Deutsches Institut für Wirtschaftsforschung https://web.archive.org/web/20180416001246/https://www.diw.de/documents/publikationen/73/diw_01.c.440963.de/diw_datadoc_2014-072.pdf.

Fares, R.L., Webber, M.E., 2017. The impacts of storing solar energy in the home to reduce reliance on the utility. Nat. Energy 2, 17001, http://dx.doi.org/10.1038/nenergy.2017.1.

Fitzgerald, G., Mandel, J., Morris, J., Touati, H., 2015. The economics of battery energy storage. https://web.archive.org/web/20181129064043/https://www.rmi.org/wp-content/uploads/2017/03/RMI-TheEconomicsOfBatteryEnergyStorage-FullReport-FINAL.pdf.

German Federal Ministry for Economic Affairs and Energy (BMWi), 2018. Energiedaten: Gesamtausgabe. Official energy statistics for Germany https://web.archive.org/web/20190121112836/https://www.bmwi.de/Redaktion/EN/Artikel/Energy/energy-data.html.

Goteti, N.S., Hittinger, E., Williams, E., 2017. How much wind and solar are needed to realize emissions benefits from storage? Energy Syst., http://dx.doi.org/10.1007/s12667-017-0266-4.

Hartner, M., Permoser, A., 2018. Through the valley: the impact of PV penetration levels on price volatility and resulting revenues for storage plants. Renew. Energy 115, 1184–1195, http://dx.doi.org/10.1016/j.renene.2017.09.036.

Hirth, L., 2013. The market value of variable renewables: the effect of solar wind power variability on their relative price. Energy Econ. 38, 218–236, http://dx.doi.org/10.1016/j.eneco.2013.02.004.

Hittinger, E., Azevedo, I.M.L., 2017. Estimating the quantity of wind and solar required to displace storage-induced emissions. Environ. Sci. Technol. 51 (21), 12988–12997, http://dx.doi.org/10.1021/acs.est.7b03286.

Huber, M., Dimkova, D., Hamacher, T., 2014. Integration of wind and solar power in Europe: assessment of flexibility requirements. Energy 69, 236–246, http://dx.doi.org/10.1016/j.energy.2014.02.109.

International Energy Agency, 2014. Linking Heat and Electricity Systems-Cogeneration and District Heating and Cooling Solutions for a Clean Energy Future. OECD/IEA https://web.archive.org/web/20170710065103/http://www.iea.org/publications/freepublications/publication/LinkingHeatandElectricitySystems.pdf.

International Energy Agency, 2018. Status of Power System Transformation 2018: Advanced Power Plant Flexibility. OECD/IEA.

Lazard, 2016. Lazard's Levelized Cost of Storage-Version 2.0. https://web.archive.org/web/20181013102141/https://www.lazard.com/media/438042/lazard-levelized-cost-of-storage-v20.pdf.

Luderer, G., Pietzcker, R.C., Carrara, S., de Boer, H.S., Fujimori, S., Johnson, N., Mima, S., Arent, D., 2017. Assessment of wind and solar power in global low-carbon energy scenarios: an introduction. Energy Econ. 64, 542–551, http://dx.doi.org/10.1016/j.eneco.2017.03.027.

Lueken, R., Apt, J., 2014. The effects of bulk electricity storage on the PJM market. Energy Syst. 5 (4), 677–704, http://dx.doi.org/10.1007/s12667-014-0123-7.

Lund, P.D., Lindgren, J., Mikkola, J., Salpakari, J., 2015. Review of energy system flexibility measures to enable high levels of variable renewable electricity. Renew. Sustain. Energy Rev. 45, 785–807, http://dx.doi.org/10.1016/j.rser.2015.01.057.

Meurer, A., Smith, C.P., Paprocki, M., Čertík, O., Kirpichev, S.B., Rocklin, M., Kumar, A., Ivanov, S., Moore, J.K., Singh, S., Rathnayake, T., Vig, S., Granger, B.E., Muller, R.P., Bonazzi, F., Gupta, H., Vats, S., Johansson, F., Pedregosa, F., Curry, M.J., Terrel, A.R., Roučka, v., Saboo, A., Fernando, I., Kulal, S., Cimrman, R., Scopatz, A., 2017. SymPy: symbolic computing in Python. PeerJ Comput. Sci. 3, e103, http://dx.doi.org/10.7717/peerj-cs.103.

Nyamdash, B., Denny, E., 2013. The impact of electricity storage on wholesale electricity prices. Energy Policy 58, 6–16, http://dx.doi.org/10.1016/j.enpol.2012.11.033.

Nykvist, B., Nilsson, M., 2015. Rapidly falling costs of battery packs for electric vehicles. Nat. Clim. Chang. 5, 329, http://dx.doi.org/10.1038/nclimate2564.

Palizban, O., Kauhaniemi, K., 2016. Energy storage systems in modern grids-matrix of technologies and applications. J. Energy Storage 6, 248–259, http://dx.doi.org/10.1016/j.est.2016.02.001.

Pena-Bello, A., Burer, M., Patel, M.K., Parra, D., 2017. Optimizing PV and grid charging in combined applications to improve the profitability of residential batteries. J. Energy Storage 13, 58–72, http://dx.doi.org/10.1016/j.est.2017.06.002.

Prognos AG, 2012. Die Energieperspektiven für die Schweiz bis 2050. Energienachfrage und Elektrizitätsangebot in der Schweiz 2000-2050 https://web.archive.

org/web/20190121112349/http://www.bfe.admin.ch/themen/00526/00527/06431/index.html?lang=en&dossier_id=06421.

REN21, Renewable Energy Policy Network for the 21st Century, 2018. Renewables 2017 Global Status Report. REN21 Secretariat, Paris https://web.archive.org/web/20190116162925/http://www.ren21.net/wp-content/uploads/2017/06/17-8399_GSR_2017_Full_Report_0621_Opt.pdf.

RTE Réseau de transport d'électricité, 2016. 2015 Bilan électrique (French power balance). https://web.archive.org/web/20171215061623/http://www.rte-france.com:80/sites/default/files/2015_bilan_electrique.pdf.

Schill, W.-P., Zerrahn, A., 2018. Long-run power storage requirements for high shares of renewables: results and sensitivities. Renew. Sustain. Energy Rev. 83, 156–171, http://dx.doi.org/10.1016/j.rser.2017.05.205.

Schmidt, O., Hawkes, A., Gambhir, A., Staffell, I., 2017. The future cost of electrical energy storage based on experience rates. Nat. Energy 2, 17110, http://dx.doi.org/10.1038/nenergy.2017.110.

Soini, M.C., Master's thesis, 2015. Impact of Large-Scale Energy Storage on the Least-Cost State of Power Systems. Chalmers University of Technology https://web.archive.org/web/20170815025519/http://publications.lib.chalmers.se/records/fulltext/219211/219211.pdf.

Soini, M.C., Parra, D., Patel, M.K., 2019. Disaggregation of energy storage operation by timescales. J. Energy Storage 23, 480–494, http://dx.doi.org/10.1016/j.est.2019.04.005.

State of California, 2010. Assembly Bill No. 2514: Energy Storage System Procurement Targets from Publicly Owned Utilities. https://web.archive.org/web/20180517214002/http://leginfo.legislature.ca.gov/faces/billNavClient.xhtml?bill_id=200920100AB2514.

Stephan, A., Battke, B., Beuse, M., Clausdeinken, J., Schmidt, T., 2016. Limiting the public cost of stationary battery deployment by combining applications. Nat. Energy 1, 16079, http://dx.doi.org/10.1038/nenergy.2016.79.

Tortora, A.C., 2014. The Case for Energy Storage: The Perspective of the TSO. Presentation Slides, Energy Storage World Forum 2014, London https://web.archive.org/web/20140411162915/http://files.energystorageforum.com:80/eswf_2014_day1/1_9_Anna_Carolina_Tortora_TERNA_STORAGE.pdf.

Wilson, I.A.G., Barbour, E., Ketelaer, T., Kuckshinrichs, W., 2018. An analysis of storage revenues from the time-shifting of electrical energy in Germany and Great Britain from 2010 to 2016. J. Energy Storage 17, 446–456, http://dx.doi.org/10.1016/j.est.2018.04.005.